Molecular Pharmacology Fast Forward. Published on April 29, 2009 as doi:10.1124/mol.109.056085
This article has not been copyedited and formatted. The final version may differ from this version.

MOL 56085

Apratoxin A reversibly inhibits the secretory pathway by preventing cotranslational translocation

Yanxia Liu, Brian K. Law, and Hendrik Luesch

Department of Medicinal Chemistry, University of Florida, 1600 SW Archer Road, Gainesville, Florida 32610, USA (Y.L., H.L.); and Department of Pharmacology & Therapeutics, University of Florida, 1376 Mowry Road, Gainesville, Florida 32610, USA (B.K.L.)

Molecular Pharmacology Fast Forward. Published on April 29, 2009 as DOI: 10.1124/mol.109.056085
This article has not been copyedited and formatted. The final version may differ from this version.

MOL 56085

Running title: The mode of action of apratoxin A

Address correspondence to: Hendrik Luesch, Department of Medicinal Chemistry, University of Florida, 1600 SW Archer Road, P.O. Box 100485, Gainesville, Florida 32610, USA; Tel.: (352) 273-7738, Fax: (352) 273-7741; Email: luesch@cop.ufl.edu.

Number of text pages: 42
Number of tables: 1
Number of figures: 6
Number of references: 40
Number of words in the *Abstract*: 146
Number of words in the *Introduction*: 409
Number of words in the *Discussion*: 765

ABBREVIATIONS: BIP, heat shock 70kDa protein 5; CALR, calreticulin; CANX, calnexin; ConA, concanavalin A; DTT, dithiothreitol; ER, endoplasmic reticulum; FBS, fetal bovine serum; FGFR, fibroblast growth factor receptor; GI_{50}, concentration at which the cell growth is inhibited by 50%; GlcNAc, *N*-acetylglucosamine; gp130, interleukin 6 signal transducer; HER-2, ERBB2 (v-erb-b2 erythroblastic leukemia viral oncogene homolog 2); HRP, horse radish peroxidase; HYOU1, hypoxia up-regulated 1; IC_{50}, concentration at which the cell viability is 50%; IGF1R-β: insulin-like growth factor 1b receptor; IL-6, interleukin-6; iTRAQ, isobaric tag for relative and absolute quantitation; JAK, janus kinase; JAK/STAT: janus kinase/signal transducer and activator of transcription; LC-MS/MS, liquid chromatography-mass spectrometry/mass spectrometry; c-MET, hepatocyte growth factor receptor; NCI, National Cancer Institute; PBS, phosphate buffered saline; PDGFR-β, platelet-derived growth factor receptor, beta polypeptide; PDI, protein disulfide isomerase; RTKs, receptor tyrosine kinases; RT-qPCR, quantitative polymerase chain reaction after reverse transcription; RPN1, ribophorin I; SDS-PAGE, SDS polyacrylamide gel electrophoresis; siRNAs, small interfering RNAs; SPARC, secreted protein osteonectin; SRP, signal recognition particle; STAT3, signal transducer and activator of transcription 3; Sulfo-NHS-SS-Biotin, sulfosuccinimidyl-2-(biotinamido)ethyl-1,3-dithiopropionate; VCAM1, vascular cell adhesion molecule 1; VEGFR2, vascular endothelial growth factor receptor-2.

Molecular Pharmacology Fast Forward. Published on April 29, 2009 as DOI: 10.1124/mol.109.056085
This article has not been copyedited and formatted. The final version may differ from this version.

ABSTRACT

Apratoxin A is a potent cytotoxic marine natural product that rapidly inhibits STAT3 phosphorylation by an undefined mechanism. We have used biochemical and proteomics approaches to illuminate upstream molecular events. Apratoxin A inhibits JAK/STAT signaling through rapid downregulation of interleukin 6 signal transducer (gp130). Apratoxin A also depletes cancer cells of several cancer-associated receptor tyrosine kinases by preventing their N-glycosylation, leading to their rapid proteasomal degradation. A proteomics approach revealed that several proteins in the endoplasmic reticulum (ER), the site of N-glycoprotein synthesis, are downregulated upon apratoxin A exposure. Using *in vitro* cell free systems we demonstrated that apratoxin A prevents cotranslational translocation of proteins destined for the secretory pathway. This process is reversible in living cells. Our study indicates that apratoxins are new tools to study the secretory pathway and raises the possibility that inhibition of cotranslational translocation may be exploited for anticancer drug development.

Molecular Pharmacology Fast Forward. Published on April 29, 2009 as DOI: 10.1124/mol.109.056085
This article has not been copyedited and formatted. The final version may differ from this version.

Natural products have established a strong position as leads for drug discovery and as tools to study gene function and biological processes (Newman, 2008). For many natural products, their mechanism of action is unknown, hampering drug development and limiting their use as tool compounds in chemical biology. The exploration of marine organisms as a source of bioactive substances has been particularly prolific in recent years (Fenical and Jensen, 2006; Blunt et al., 2008). Among those, marine cyanobacteria have emerged as major producers of bioactive secondary metabolites (Gerwick et al., 2001). For example, we recently described some of the most potent natural elastase inhibitors (Taori et al., 2007) and one of the most potent class I histone deacetylase inhibitors (Taori et al., 2008; Ying et al. 2008) known, isolated from Floridian marine cyanobacteria. While structure-based approaches led to their target identification, for other natural products the target is less obvious, necessitating extensive mechanistic studies on the cellular and molecular level to rationalize the biological activity. Recent examples are the apratoxins (Luesch et al., 2001, 2002; Gutiérrez et al, 2008; Matthew et al., 2008), a class of cytotoxic natural products which we (H.L.) originally isolated from a marine cyanobacterium from Micronesia (Luesch et al., 2001). The biological activity and intricate structure prompted synthetic chemists to undertake the total synthesis (Chen & Forsyth, 2004; Doi et al., 2006; Ma et al., 2006). Of the five natural apratoxins known to date, apratoxin A (**1**) (Figure 1A) exhibits the highest potency against various cancer cells (Luesch et al., 2001). For many cancer cell lines antiproliferative activity was found to be in the low nanomolar range (Luesch et al., 2006). We (H.L.) recently reported that apratoxin A possesses differential cytotoxicity in the NCI-60 cell line assay with a unique profile compared with standard agents (Luesch et al., 2006). Apratoxin A was shown to induce pronounced G1 cell cycle arrest and apoptosis (Luesch et al., 2006). A genomic overexpression in U2OS osteosarcoma cells revealed

Molecular Pharmacology Fast Forward. Published on April 29, 2009 as DOI: 10.1124/mol.109.056085
This article has not been copyedited and formatted. The final version may differ from this version.

that ectopic induction of FGFR signaling attenuates apratoxin A activity, which was linked to the phosphorylation of oncogenic transcription factor STAT3 at its activating site, tyrosine-705 (Luesch et al., 2006). Apratoxin A potently inhibits STAT3 (Tyr705) phosphorylation in various cell types, however, the upstream events remained elusive up to now. Here we report on the mode of action of apratoxin A, including the cause for apratoxin A-induced loss of STAT3 phosphorylation. Our results indicate that apratoxin A acts via a novel mechanism.

Materials and Methods

Cell culture. U2OS cells and MCF7 cells were cultured in Dulbecco's modified Eagle's medium (Invitrogen, Carlsbad, CA) supplemented with 10% fetal bovine serum (Hyclone, Logan, UT) at 37 ºC humidified air and 5% CO_2.

Inhibitors and reagents. Apratoxin A was obtained from the marine cyanobacterium from Guam. The isolation of apratoxin A has been described (Luesch et al., 2001). MG132 and cycloheximide were purchased from Calbiochem (Gibbstown, NJ). Chloroquine, tunicamycin and interleukin-6 (IL-6) were from Sigma-Aldrich (St. Louis, MO). Bafilomycin A_1 was from Biomol International L.P. (Plymouth Meeting, PA).

Immunoblot analysis. At a desired density (to reach ~80% confluency for control cells), U2OS cells or MCF7 cells were treated with apratoxin A (50 nM), tunicamycin (500 ng/mL), cycloheximide (1 µg/mL) or solvent controls for 1 h, 4 h, 12 h and 24 h. For washout experiments, U2OS cells were seeded in 60-mm dishes at densities from 1×10^5 to 4×10^5 cells based on different time points. The next day, cells were treated with 50 nM apratoxin A or solvent control for 1 h, 4 h, 12 h and 24 h. Following exposure to apratoxin A, growth medium was removed, cells washed once and then cultured for additional time in apratoxin A-free

Molecular Pharmacology Fast Forward. Published on April 29, 2009 as DOI: 10.1124/mol.109.056085
This article has not been copyedited and formatted. The final version may differ from this version.

medium. Whole cell lysates were collected using PhosphoSafe lysis buffer (Novagen, Madison, WI) at 1 h, 4 h, 12 h, 24 h, 48 h, 72 h and 96 h after begin of drug treatment. Nuclear proteins were separated using the NE-PER reagent (Pierce, Rockford, IL). Protein concentrations were measured using the BCA Protein Assay kit (Pierce). Lysates containing equal amounts of protein were separated by SDS-PAGE gel (4–12%), transferred to PVDF membranes, probed with antibodies and detected with the SuperSignal West Femto Maximum Sensitivity Substrate (Pierce). Anti-gp130 antibody was obtained from Millipore (Billerica, MA). Anti-phospho-STAT3 (Tyr705), anti-STAT3, anti-phospho-JAK1 (Tyr1022/1023), anti-JAK1, anti-phospho-JAK2 (Tyr1007/1008), anti-JAK2, anti-Met (25H2), anti-VEGFR2, anti-calnexin (CANX), anti-calreticulin (CALR), anti-BIP, anti-PDI, anti-β-actin, anti-β-tubulin (TUBB), anti-rabbit, and anti-mouse antibodies were from Cell Signaling (Beverly, MA). Anti-Oct-1 (C-21), anti-PDGFR-β, anti-IGF1R-β (C-20), anti-FGFR2, and anti-goat antibodies were from Santa Cruz Biotechnology, Inc (Santa Cruz, CA). Anti-HER-2 antibody was from Thermo Scientific (Waltham, MA). Anti-*O*-GlcNAc (MAb CTD 110.6) and goat anti-mouse IgM (μ) antibodies were from Pierce. Anti-TXNDC5, anti-ribophorin 1 (RPN1) and anti-SPARC antibodies were from Abcam (Cambridge, MA).

RNA interference. Nontargeting control siRNA and siRNA reagents targeting *gp130* were obtained from Applied Biosystems (Foster City, CA). 4.0×10^5 U2OS cells were seeded in 60-mm dishes and transfected the next day with 10 nM, 20 nM and 50 nM of siRNA using siLentFect (Bio-Rad, Hercules, CA). Following 48 h incubation, whole cell protein lysates were harvested by using PhosphoSafe lysis buffer and used for immunoblot analysis.

RT-qPCR. 1.0×10^5 U2OS cells were seeded in 6-well plates and transfected the next day using siLentFect (Bio-Rad) with 1.8 μg of cDNA encoding gp130 (Origene Technologies,

Molecular Pharmacology Fast Forward. Published on April 29, 2009 as DOI: 10.1124/mol.109.056085
This article has not been copyedited and formatted. The final version may differ from this version.

Rockville, MD) and vector control. CMV-*GFP* (0.2 μg) was cotransfected to monitor transfection efficiency. Following 48 h incubation, total RNA was extracted with the RNeasy Mini Kit (Qiagen, Valencia, CA). cDNA was synthesized from 2 μg of total RNA by using SuperScript II Reverse Transcriptase (Invitrogen) and Oligo(dT)$_{12\text{-}18}$ Primer (Invitrogen). Real-time PCR was performed by using 12.5 μL of TaqMan 2× universal master mix (Applied Biosystems), 1.25 μL of 20× TaqMan gene expression assay mix (Applied Biosystems), 2 μL of cDNA and 9.25 μL of sterile water, in a total volume of 25 μL per well reaction in 96-well plate (Applied Biosystems) using the ABI 7300 sequence detection systems (Applied Biosystems). The thermocycler program consisted of 2 min at 50 °C, 10 min at 95 °C, and 40 cycles of 95 °C for 15 s and 60 °C for 1 min. Each assay was carried out in triplicate. *GAPDH* expression was used as internal control for normalization.

Inhibitor treatments. U2OS cells were seeded in 60-mm dishes (4×10^5 cells/dish). The next day, cells were pretreated with MG132 (1 μM, 30 min), chloroquine (100 μM, 30 min) or NH_4Cl (20 mM, 2 h) and then exposed to apratoxin A (50 nM) or solvent control for 2 h, 4 h and 8 h. The whole cell protein lysates were harvested by using PhosphoSafe lysis buffer (Novagen) and used for immunoblot analysis.

LysoTracker experiment. 8.0×10^3 U2OS cells were seeded in a 96-well plate. The next day, cells were incubated with LysoTracker Red (Invitrogen) at 37 °C (500 nM final concentration) to label the lysosome, 30 min later the medium was removed, the cells were washed twice with phosphate buffered saline (PBS) and wells refilled with culture medium. The cells were treated with apratoxin A (10 nM, 100 nM and 1 μM) or bafilomycin A_1 (5 nM, 50 nM and 500 nM) or solvent controls for 3 h. The medium was removed, wells were refilled with PBS and images captured under a fluorescence microscope (Eclipse Ti, Nikon, Japan).

Molecular Pharmacology Fast Forward. Published on April 29, 2009 as DOI: 10.1124/mol.109.056085
This article has not been copyedited and formatted. The final version may differ from this version.

Chromaffin granule (including V-ATPase) isolation and V-ATPase assay. The isolation of V-ATPase containing chromaffin granules has been adapted from published procedures (Nelson et al., 1988). The V-ATPase assay was performed using an ATPase assay kit according to the manufacturer's instructions (Innova Biosciences, Cambridge, UK).

Enzymatic protein deglycosylation. U2OS whole cell lysates (10 µg), 1 µL of 10× glycoprotein denaturing buffer and H_2O were mixed for a total volume of 10 µL. Glycoproteins were denatured by heating at 100 °C for 10 min. The enzymatic reactions were carried out in a volume of 20 µL by adding 2 µL 10× reaction buffer, 2 µL 10% NP40, 5 µL H_2O and 1.0 µL PNGase F (New England Biolabs, Ipswich, MA). The reaction mixture was incubated at 37 °C for 1 h. Deglycosylation by PNGase F was assessed by immunoblot analysis and compared with lysates derived from U2OS cells treated with 50 nM apratoxin A, 500 ng/mL tunicamycin or solvent control for 12 h.

Total protein analysis by silver staining. Silver staining was performed according to the protocol of Bio-Rad Silver Stain (Bio-Rad).

Plasma membrane protein enrichment. 1.8×10^7 U2OS cells were treated with apratoxin A (50 nM) or solvent control for 12 h, washed twice with PBS, suspended in 10 mM HEPES-NaOH (pH 7.5), 0.25 M sucrose and protease inhibitor cocktail (Pierce). The suspension was placed in a 2 mL Dounce homogenizer (Fisher Scientific, Pittsburgh, PA), fitted with a tight (Type B) pestle and subjected to 10–20 down strokes of the pestle until approximately 95% of the cells were broken. The cell lysates were then centrifuged at 3,000 × *g* for 10 min to remove large cell debris and nuclei. The supernatant was layered on a discontinuous sucrose density gradient, containing layers of 15, 30, 45, and 60% sucrose (w/v) in 10 mM Hepes-NaOH (pH 7.5) and centrifuged at 100,000 × *g* (SW 28 rotor) overnight at 4 ºC. Resultant fractions were

Molecular Pharmacology Fast Forward. Published on April 29, 2009 as DOI: 10.1124/mol.109.056085
This article has not been copyedited and formatted. The final version may differ from this version.

diluted 4-fold with distilled water and centrifuged at 200,000 × *g* (70 Ti rotor) for 2 h to obtain plasma membrane-rich pellets which were resuspended in PhosphoSafe lysis buffer, analyzed by SDS-PAGE gel followed by silver staining or immunoblot analysis.

N-glycoprotein enrichment. U2OS cells were treated with apratoxin A (50 nM) or solvent control for 12 or 24 h. Cytoplasmic proteins were extracted [50 mM HEPES, pH 8.0; 100 mM KOAc, 5 mM $MgCl_2$, 100 µg/mL digitonin, protease inhibitor tablet (Roche, Indianapolis, IN)] for 10 min on ice. Cells were washed (50 mM HEPES, pH 8.0; 100 mM KOAc, 5 mM $MgCl_2$, protease inhibitor), membrane proteins were extracted (50 mM HEPES, pH 8.0; 100 mM KOAc, 5 mM $MgCl_2$, 1% Triton X-100, protease inhibitor), the insoluble material was removed by centrifugation for 10 min at 3,000 × *g*, and the supernatant was incubated with immobilized Concanavalin A agarose (Pierce) to bind cellular glycoproteins. The glycoproteins were eluted with 0.5 M methyl-α-D-mannopyranoside and analyzed by SDS-PAGE gel.

Cell surface protein enrichment. Cell surface proteins were isolated according to the instruction of Pierce Cell Surface Protein Isolation Kit (Pierce, Rockford, IL) similarly as described (Nunomura et al., 2005). To compare degradation rates of pre-existing gp130, U2OS cells (1×10^6 cells) were seeded in 10-cm dishes, biotinylated at 4 °C using EZ-Link Sulfo-NHS-SS-Biotin and incubated for 1 h, 2 h and 4 h with apratoxin A (50 nM) or solvent control (0.25% EtOH) at 37 °C. Cells were lysed with Lysis buffer (310 µL) and an aliquot (10 µL) analyzed by immunoblot analysis for total gp130 and STAT3. Labeled proteins isolated with Immobilized NeutrAvidin Gel (agarose beads) and eluted with 50 mM DTT (450 µL). The isolated proteins were precipitated with acetone, resuspended in PhosphoSafe lysis buffer and analyzed by SDS-PAGE gel followed by immunoblot analysis. In an alternative procedure, to quantify protein expression changes by proteomics, 4.5×10^6 U2OS cells were seeded in T225 cm^2 flasks and the

Molecular Pharmacology Fast Forward. Published on April 29, 2009 as DOI: 10.1124/mol.109.056085
This article has not been copyedited and formatted. The final version may differ from this version.

next day cells were treated with 50 nM apratoxin A or solvent control for 1 h, 4 h, 12 h and 24 h. Then the cells were labeled with EZ-Link Sulfo-NHS-SS-Biotin; for each time point two flasks were used for each treatment. Cells were subsequently lysed with 510 µL Lysis Buffer. 10 µL cell lysate were used for biotinylation confirmation by Western blot analysis using horseradish peroxidase conjugated streptavidin (Pierce). The remainder of the labeled proteins was then isolated with Immobilized NeutrAvidin Gel (agarose beads). The bound proteins were eluted with 450 µL 50 mM DTT.

Proteomics studies. a) ***iTRAQ labeling and LC-MS analysis.*** Proteins were precipitated from 100 µL samples using acetone, and suspended with PhosphoSafe buffer to measure protein concentration, and enrichment of cell surface proteins was confirmed by immunoblot analysis and silver staining (Bio-Rad). Based on the measured concentration, 250 µL of sample was used for iTRAQ labeling. All the procedures were performed according to the manufacturer's instruction (Applied Biosystems). Briefly, proteins were precipitated by acetone precipitation. Each protein pellet was lysed with 20 µL of 0.5 M triethylammonium bicarbonate and denatured with 0.1 % SDS. The disulfide bonds of the proteins were reduced by 2 µL of 50 mM tris-(2-carboxyethyl)-phosphine, and the cysteine group was blocked by 1 µL of 200 mM methyl methanethiosulfonate in isopropanol. After the proteins were digested by trypsin (Promega) overnight at 37 °C, the protein digests were labeled with the iTRAQ™ Reagents 8plex, and samples of labeled peptides from all 8 different conditions were combined. The combined sample mixture was diluted into 0.1% trifluoricacetic acid, followed by loading on a MacroSpin Vydac C18 reverse phase minicolumn (Nestgroup Inc., USA). The eluates were dried down and dissolved in strong cation exchange (SCX) solvent A (25% v/v acetonitrile, 10 mM ammonium formate, pH 2.8). The peptides were fractionated on an Agilent HPLC system 1100 using a

Molecular Pharmacology Fast Forward. Published on April 29, 2009 as DOI: 10.1124/mol.109.056085
This article has not been copyedited and formatted. The final version may differ from this version.

polysulfoethyl A column (2.1 × 100 mm, 5 µm, 300 Å, PolyLC, Columbia, MD). Peptides were eluted at a flow rate of 200 µL/min with a linear gradient of 0–20% solvent B (25% v/v acetonitrile, 500 mM ammonium formate) over 50 min, followed by ramping up to 100% solvent B in 5 min and holding for 10 min. The absorbance at 280 nm was monitored, and a total of 14 fractions were collected. QSTAR XL system (Applied Biosystems) was used in reverse phase LC-MS/MS. Each SCX fraction was lyophilized and redissolved in solvent A (3% acetonitrile v/v, 0.1% acetic acid v/v) plus 0.01% trifluoroacetic acid. The peptides were loaded onto a C18 capillary trap cartridge (LC Packings) and then separated on a 15-cm nanoflow C18 column (PepMap 75 µm id, 3 µm, 100 Å) (LC Packings) at a flow rate of 200 nL/min. Peptides were eluted from the HPLC column by a linear gradient from 3% solvent B (96.9% acetonitrile v/v, 0.1% acetic acid v/v) to 40% solvent B for 2 hours, followed by ramping up to 90% solvent B in 10 min. Peptides were sprayed into the orifice of the mass spectrometer, which was operated in an information-dependent data acquisition mode where a MS scan followed by three MS/MS scans of three highest abundance peptide ions were acquired in each cycle. ***b) Data analysis.*** The MS/MS data was processed by a thorough search considering biological modifications against the IPI human database (downloaded on August 8, 2007) using the Paragon algorithm (Shilov et al., 2007) of ProteinPilot v2.0.1 software suite (Applied Biosystems). Fixed modification of methyl methanethiosulfate labeled cysteine, fixed iTRAQ modification of free amine in the N-terminus and lysine, and variable iTRAQ modifications of tyrosine were considered. Parameters such as trypsin digestion, precursor mass accuracy and fragment ion mass accuracy are built-in settings of the software. The raw peptide identification results from the Paragon™ Algorithm were further processed by the ProGroup™ Algorithm. For protein relative quantification using iTRAQ, only MS/MS spectra unique to a particular protein and where the sum of the signal-to-

Molecular Pharmacology Fast Forward. Published on April 29, 2009 as DOI: 10.1124/mol.109.056085
This article has not been copyedited and formatted. The final version may differ from this version.

noise ratio for all of the peak pairs greater than nine were used for quantification (software default settings, Applied Biosystems).

Cell viability assay. U2OS cells were seeded in clear-bottom 96-well plates (5×10^3/well), and treated 24 h later with various concentrations of apratoxin A (1 nM to 1 µM) or solvent control. 1 h, 4 h, 12 h and 24 h after treatment, culture medium was aspirated, cells rinsed once with fresh medium and wells refilled with fresh medium. After a total of 48 h of incubation, cell viability was measured using MTT according to the manufacturer's instructions (Promega, Madison, WI). In parallel, a dose-response analysis was carried out after continuous exposure of cells to apratoxin A (48 h).

Caspase 3/7 assays. U2OS cells were plated in solid-white 96-well assay plate (5×10^3/well). The same treatment and washout steps as for the cell viability assay were performed. After another 24 h of incubation, caspase 3/7 activity was measured by using Caspase-Glo 3/7 assay (Promega). Caspase-Glo 3/7 reagent was prepared immediately before use by mixing the lysis buffer and luciferase substrate and equilibrated to room temperature. The assay plate was also equilibrated to room temperature (~10 min). The same volume of Caspase-Glo 3/7 reagent as culture medium was added to each well (100 µL) and the plate was mixed on a plate shaker for ~1 min and incubated at room temperature for 30 min. The luminescence was read in a luminescence plate reader (SpectraMax M5, Molecular Devices, Sunnyvale, CA).

***In vitro* translation.** The translation reactions containing 17.5 µL of nuclease-treated rabbit reticulocyte lysate (Promega), 0.5 µL of amino acid mix (minus methionine, 1 mM), 2.0 µL of canine pancreatic microsomal membranes (Promega), 1.0 µL of RNA substrate in nuclease-free water (β-lactamase or α-factor mRNA at 0.1 µg/µL), 1 µL mixture of water and apratoxin A (0.875 µL water; 0.125 µL of 20 nM, 200 nM, 2 µM, 20 µM, 200 µM, 2 mM apratoxin A or

Molecular Pharmacology Fast Forward. Published on April 29, 2009 as DOI: 10.1124/mol.109.056085
This article has not been copyedited and formatted. The final version may differ from this version.

solvent control), 1.5–2.0 µL of L-[^{35}S]methionine (EasyTag^{TM}, 15–20 µCi; PerkinElmer, Waltham, MA) and nuclease-free water to a final volume of 25 µL were incubated at 30 °C for 60 min. One reaction without canine pancreatic microsomal membranes was included. 5 µL of the reaction was used for analyzing the results of translation and processing by SDS-PAGE (20%) and autoradiography.

Coupled *in vitro* transcription/translation. Human PDGFR-β cDNA plasmid (vector pCMV6-XL5) was obtained from Origene Technologies. *In vitro* transcription/translation was carried out by using TNT T7 quick coupled transcription/ translation systems (Promega). The reactions containing 20 µL of T7 TNT quick master mix, 1 µL of plasmid DNA (1 µg/µL), 1.5 µL canine pancreatic microsomal membranes (Promega), 1 µL mixture of water and apratoxin A (0.875 µL water; 0.125 µL of 20 nM, 200 nM, 2 µM, 20 µM, 200 µM, 2 mM apratoxin A or solvent control), 1.5–2.0 µL of L-[^{35}S]methionine (EasyTag^{TM}, 15–20 µCi, PerkinElmer) and nuclease-free water to a final volume of 25 µL were incubated at 30 °C for 90 min. One reaction without canine pancreatic microsomal membranes was also included. 5 µL of the reaction was used for analyzing the results of translation and processing by SDS-PAGE (7.5%) and autoradiography.

Protease protection assay. A solution of 1 mg/mL of proteinase K (Roche) in Tris-HCl (pH 7.5) was preincubated at 37 °C for 15 min to degrade contaminating lipases. 9.5 µL of translation reactions were chilled on ice and $CaCl_2$ was added to 10 mM. 1 µL of treated proteinase K was added to the translation reactions (10 µM apratoxin A and solvent control) in the presence or absence of 1% Triton X-100. The reactions were incubated at 0 °C for 30 min and stopped by the addition of 2 µL of 50 mM phenylmethylsulfonyl fluoride in ethanol and immediately transferred

Molecular Pharmacology Fast Forward. Published on April 29, 2009 as DOI: 10.1124/mol.109.056085
This article has not been copyedited and formatted. The final version may differ from this version.

to boiling SDS-PAGE loading buffer and then analyzed by SDS-PAGE (20%) and autoradiography.

Results

Apratoxin A inhibits signaling through STAT3 by depleting cancer cells of gp130. The phosphorylation of STAT3 at residue Tyr-705 has been thought to be required for STAT3 translocation from the cytoplasm to the nucleus and subsequent activation of STAT3 target gene transcription (Zhong et al, 1994), although alternative mechanisms have recently been implicated (Yuan et al., 2005, Liu et al., 2005). Thus, we first tested the hypothesis that apratoxin A prevents STAT3 nuclear translocation. We prepared nuclear extracts from U2OS osteosarcoma cells treated with apratoxin A for different times and assessed STAT3 content in the nucleus by immunoblot analysis. After 4 h, STAT3 levels were significantly decreased in the nucleus and effects were even more pronounced at later time points (Figure 1B), supporting the proposed STAT3 inhibition. To determine if the inhibition occurred at the level of STAT3 we turned to upstream components of signaling pathways that converge at STAT3. Since JAK kinases are canonical STAT3 (Tyr705) phosphorylating kinases which require phosphorylation themselves to be active, we assessed the phosphorylation status of the catalytic residues of JAK1 (Tyr1022/1023) and JAK2 (Tyr1007/1008) by immunoblot analysis with phospho-specific antibodies. Phosphorylation of both JAKs decreased over time, while total protein levels were unaffected (Figure 1C). Next, we determined whether apratoxin A not only inhibited baseline STAT3 phosphorylation arising from FBS in the growth medium, but also upon cytokine activation using interleukin-6 (IL-6), a cytokine that strongly stimulates JAK-STAT3 signaling (Chen et al., 2006). Using cells that had been serum-starved for 48 h, we first established the

Molecular Pharmacology Fast Forward. Published on April 29, 2009 as DOI: 10.1124/mol.109.056085
This article has not been copyedited and formatted. The final version may differ from this version.

optimal IL-6 concentration (10 ng/mL) and response time (20 min) in U2OS cells (Figure 1D). Apratoxin A also inhibited IL-6 induced STAT3 (Tyr705) phosphorylation; however, approximately 4 h of pre-treatment were required for full inhibitory effect (Figure 1E), suggesting that another event had to occur first. Consequently, we investigated the effect of apratoxin A on interleukin 6 signal transducer (gp130), the cytokine receptor that is the shared signaling subunit of the IL-6 type cytokines (Heinrich et al., 2003). Using immunoblot analysis, we tested the protein levels of gp130 and noticed its rapid depletion in a time-dependent manner upon treatment with 50 nM apratoxin A (Figure 1F). After 4 h, the band corresponding to gp130 in the control was already reduced by >90% compared with control, which would explain the apratoxin A-induced inhibition of STAT3 phosphorylation. Furthermore, this time course closely paralleled the effect of apratoxin A on STAT3 (Tyr705) phosphorylation, in agreement that both events are mechanistically related. To ascertain that this is the case, we obtained two independent small interfering RNAs (siRNAs) specifically targeting the *gp130* transcript. After verifying knockdown efficiency (>90% at 50 nM, Figure 1G) we examined STAT3 phosphorylation status at Tyr705 and observed abrogation of Tyr705 phosphorylation in a si*gp130* concentration-dependent manner while total STAT3 levels remained steady (Figure 1G).

Mechanism of gp130 degradation. To determine if apratoxin A triggers gp130 abrogation on the transcript level, we carried out RT-qPCR. TaqMan analysis indicated that apratoxin A had no significant effect on the amount of *gp130* mRNA within the 24 h measured (Figure 2A). This data suggested that the downregulation had to occur on the protein level and that apratoxin A affects protein synthesis or degradation. The two major mechanisms of protein degradation are proteasomal and lysosomal degradation. To determine the contribution of both pathways to the apratoxin A-mediated gp130 degradation, we uncoupled them by individual inhibition. First, we

Molecular Pharmacology Fast Forward. Published on April 29, 2009 as DOI: 10.1124/mol.109.056085
This article has not been copyedited and formatted. The final version may differ from this version.

used the proteasome inhibitor MG132 at a previously determined effective concentration in U2OS cells [at IC_{90} (48 h) = 1 μM]. We pretreated U2OS cells with MG132 for 30 min before apratoxin A addition (50 nM) for 2, 4 and 8 h, then extracted cellular proteins and carried out immunoblot analysis for gp130 (Figure 2B). Comparison of gp130 levels in MG132-pretreated cells with levels in cells that had only been treated with apratoxin A demonstrated a marginal rescue at 4 and 8 h arising from proteasome inhibition. Importantly, a band of slightly lower molecular weight became apparent, suggesting that a not fully processed gp130 protein or fragment of gp130 was stabilized upon proteasome inhibitor treatment (Figure 2B). Next, we used ammonium chloride (20 mM) to increase the pH in the lysosome to inhibit lysosomal protein degradation (Kawai et al., 2007). When cells were pretreated with NH_4Cl for 2 h, the degradation of gp130 was partially inhibited or slowed (Figure 2C), suggesting that lysosomal degradation is another fate of the fully processed and functional receptor, as previously shown (Blanchard et al., 2001). However, the immunoreactive protein of lower molecular weight was unaffected by NH_4Cl. The lysosome inhibitor chloroquine (100 μM) had a similar effect but may have accelerated degradation of the faster migrating gp130 band (Figure 2D). Rescue effects on STAT3 (Tyr705) phosphorylation were small (Figures 2C and 2D). One possible explanation for this marginal shift in activity is also that apratoxin A may trigger lysosomal degradation which can be overcome by extending the receptor's half-life. In the lysosome the major enzyme regulating the pH, V-ATPase, is already targeted by other anticancer drugs in development (Bowman & Bowman, 2005). Pharmacological inhibition, e.g., with the natural product bafilomycin A_1, has been shown to increase the intra-lysosomal pH and pH of other acidic V-ATPase-containing compartments such as endosomes, interfering with autophagy (Johnson et al., 1993). Elevating endosome pH has been reported to slow receptor externalization, but not

Molecular Pharmacology Fast Forward. Published on April 29, 2009 as DOI: 10.1124/mol.109.056085
This article has not been copyedited and formatted. The final version may differ from this version.

internalization, and ultimately downregulate receptor signaling (Johnson et al., 1993). To compare the effects of apratoxin A and bafilomycin A_1 we detected acidic compartments using LysoTracker Red, which labels the lysosome red if acidic pH is not compromised. Expectedly, bafilomycin A_1 alkalinizes the lysosome by V-ATPase inhibition, so that the fluorescence disappeared (Figure 2E). In agreement with the NH_4Cl experiment, apratoxin A does not increase the pH compared with vehicle treatment (Figure 2E), indicating a different mode of action compared with the bafilomycins. We confirmed via enzymatic assay that apratoxin A does not affect activity of V-ATPase (purified from bovine adrenal glands), using bafilomycin A_1 as a positive control.

Apratoxin A downregulates several cancer-associated receptors. To determine the specificity with which apratoxin A downregulates gp130, we assessed the effects of apratoxin A on other receptors, particularly receptor tyrosine kinases (RTKs) known to be overexpressed in various cancers and which are validated targets for anticancer therapy (Baselga, 2006). Apratoxin A (50 nM) rapidly downregulated protein levels of c-MET, HER-2, PDGFR-β and IGF1R-β within several hours of treatment (Figure 3A). Upon closer inspection of the Western blots, we consistently noticed immunoreactive bands of slightly lower molecular weight for apratoxin A treated cells, as seen for gp130. These faster migrating bands could be explained by the presence of the corresponding receptors with lower degree or lack of posttranslational modification. Since these receptors are usually glycosylated, we suspected that the molecular weight difference could arise from deglycosylated receptors which are more rapidly degraded (since the lack of glycosylation leads to misfolding), resulting in a less intense band. To test this hypothesis, we treated U2OS cells with tunicamycin (500 ng/mL), a broad-spectrum inhibitor of N-linked glycosylation by inhibiting GlcNAc phosphotransferase which catalyzes the transfer of

Molecular Pharmacology Fast Forward. Published on April 29, 2009 as DOI: 10.1124/mol.109.056085
This article has not been copyedited and formatted. The final version may differ from this version.

N-acetylglucosamine-1-phosphate from UDP-*N*-acetylglucosamine to dolichol phosphate in the first step of glycoprotein synthesis. Tunicamycin had an identical effect on the receptor levels, and a similar time course, as apratoxin A (Figure 3B). The immunoreactive lower band corresponded to the band that was observed with apratoxin A, and in both cases this band was faint. Even tunicamycin's effect on STAT3 (Tyr705) phosphorylation paralleled the effect of apratoxin A. This band was slightly lower than the band arising from treatment of control lysates with the endoglycosidase PNGase F (Supplementary Figure S1), which may be due to additional protein modifications in control cells but not in apratoxin A or tunicamycin treated cells. For comparison, the general protein synthesis inhibitor cycloheximide (1 μg/mL) decreased the levels of the receptors without inducing a second band with higher electrophoretic mobility (Figure 3C). Apratoxin A (50 nM) cotreatment with neither tunicamycin (500 ng/mL) nor cycloheximide (1 μg/mL) accelerated gp130 downregulation (Figure 3D), and the lack of apparent cooperative effects at these high concentrations may suggest that apratoxin A only affects receptor synthesis and not additionally receptor degradation. To directly demonstrate that apratoxin A does not alter the degradation rate of pre-existing receptors such as gp130, we biotinylated cell surface proteins, then treated with apratoxin A, isolated biotinylated proteins at various time points using NeutrAvidin Gel, and imunoblotted for gp130. Cell surface gp130 derived from apratoxin A-treated U2OS cells disappeared at the same rate as cell surface gp130 from vehicle-treated cells (Figure 3E).

Since we were unable to detect significant protein levels of fibroblast growth factor receptors (FGFRs) and VEGFR2, and to assess cell type specificity, we determined if apratoxin A can reduce expression levels of these cancer-associated receptors linked also to angiogenesis in the MCF7 breast cancer cell line (Garvin et al., 2005). Apratoxin A (50 nM) strongly downregulated

Molecular Pharmacology Fast Forward. Published on April 29, 2009 as DOI: 10.1124/mol.109.056085
This article has not been copyedited and formatted. The final version may differ from this version.

FGFR2 and VEGFR2 in this cell line after 12 h of exposure (Figure 3F). We subsequently isolated the plasma membrane fraction from apratoxin A-treated (12 h) and control U2OS cells by ultracentrifugation over sucrose gradients to compare total cell surface protein content. We verified receptor enrichment using PDGFR-β immunoblot analysis (Figure 3G). While we were unable to identify discernable differences in treated versus nontreated whole-cell lysates by silver staining (Figure 3G, lanes 1 vs. 2), several but not all plasma membrane protein levels were reduced upon apratoxin A treatment (Figure 3G, lanes 3 vs. 4, indicated by *), suggesting a selective effect of apratoxin A on a subset of glycosylated cell surface proteins. To test if the effect of apratoxin A is specific to N-glycosylation, we resolved protein lysates by SDS-PAGE, carried out Western blot analysis for O-glycosylation using *O*-GlcNAc antibody. No significant differences were apparent between control lysates and those derived from cells treated with apratoxin A for 1, 4, 12 or 24 h (not shown). Conversely, lysates collected after various treatment times that were then enriched in glycoproteins through lectin-based isolation using Concanavalin A (ConA) agarose, validated by gp130 immunoblot analysis (Figure 3H), showed differences after 12 h and more pronounced after 24 h of apratoxin A treatment (Figure 3H, indicated by *). Of note, this analysis also identified changes in the 50 kDa range, which presumably are not receptors (Figure 3H). These results overall suggested that 1) apratoxin A action is specific to N-linked glycosylation, and 2) only a subset of proteins is affected.

Proteomics identifies subcellular consequences of apratoxin A treatment. To ascertain which other protein levels may be modulated by apratoxin A, we employed an iTRAQ-based proteomics approach that allows multiplexed relative protein quantification in a single LC-MS/MS experiment (Aggarwal et al., 2006). We compared protein lysates from cells treated with apratoxin A versus vehicle for 1, 4, 12 and 24 h, initially focusing on whole-cell lysates. Proteins

Molecular Pharmacology Fast Forward. Published on April 29, 2009 as DOI: 10.1124/mol.109.056085
This article has not been copyedited and formatted. The final version may differ from this version.

were extracted and precipitated, digested with trypsin and resulting peptide mixtures for different conditions individually labeled with 8-plex isobaric iTRAQ reagents and then combined to one single sample, fractionated over cation exchange resin and subjected to LC-MS/MS analysis (Figure 4A, middle). As with the silver staining of SDS-PAGE resolved whole cell lysates, this experiment failed to disclose significant differences or reproducible trends. However, since we revealed major effects on several receptors (Figure 3A), our strategy was to specifically label cell surface proteins with biotin through coupling with Sulfo-NHS-SS-Biotin (**2**) (4 ^{o}C, 30 min) after apratoxin A treatment and then to use NeutrAvidin Gel to isolate biotin-labeled and associated proteins. Tagged proteins were then eluted by DTT-mediated reductive disulfide cleavage of the biotin-containing reagent, leaving a cap behind. Downstream analysis would allow direct comparison of protein levels (Figure 4A, right). We verified labeling by blotting with HRP-conjugated streptavidin (Figure 4B), subsequently enriched biotinylated proteins using NeutrAvidin-agarose beads, reductively cleaved the biotin tag during elution, and confirmed that receptors such as gp130 have been enriched by this procedure (Figure 4C). Silver staining of SDS-PAGE gels for total protein content further showed that we enriched a minor subset of proteins. The same analysis also confirmed that there are no apparent differences between whole-cell lysates treated with vehicle or apratoxin A, while it revealed only minor differences for lysates collected after biotin-labeling of apratoxin A and vehicle-treated cells when equal amounts of protein were loaded onto the gel (Figure 4C). Taken together, apratoxin A affected only a fairly specific subset of proteins. Of note, approximately 4–6% of the original protein content was recovered each time, suggesting that proteins presumably associated with cell surface proteins were also enriched or that labeling was not entirely specific. We proceeded with the iTRAQ labeling and downstream analysis as described above (Figure 4A, right). Peptides

Molecular Pharmacology Fast Forward. Published on April 29, 2009 as DOI: 10.1124/mol.109.056085
This article has not been copyedited and formatted. The final version may differ from this version.

were identified by LC-MS/MS analysis, and numerous time-dependent changes were observed. At a confidence level of 95% with at least one peptide hit at each of the time points we identified 476 proteins, 66 of which showed at least a 2-fold change at one of the four time points.

Most of the proteins of lower expression in the apratoxin A-treated samples could easily be classified into receptor- or membrane-associated proteins, protein disulfide isomerase (PDI) related proteins which can serve or interact with chaperones, and other proteins that mainly reside in the endoplasmic reticulum (ER) (Table 1, see Supplementary Table S1 for complete list). However, gp130 and other previously identified downregulated receptors were not identified by this approach. This may have been caused by inefficient labeling of receptors with the iTRAQ reagent since some lysine amino residues may have been blocked by the cap left after biotin cleavage, miscleavage during trypsin digest (arising from lysine modification from biotinylation), or due to low expression levels. While somewhat unexpectedly on the list, several of the ER-resident proteins had been previously identified by cell surface biotinylation (Xiao et al., 1999); however, labeling was presumably also not entirely specific. Only a few proteins were reproducibly upregulated upon apratoxin A treatment (Table 1 and Supplementary Table S1) most of which are involved in general protein biosynthesis. One protein found, SRP72, is specific to the secretory pathway. SRP72 is the major protein of the signal recognition particle (SRP). The SRP complex recognizes the hydrophobic N-terminal signal sequence characteristic for secreted and membrane proteins and mediates the transport of the free ribosomes to the ER (Walter et al., 1984). The upregulation of SRP72 and other proteins required for translation is likely due to a positive feedback arising from the reduced membrane protein levels.

Downregulation of selected proteins by apratoxin A was verified by immunoblot analysis using whole-cell protein extracts (Figure 4D). Furthermore, to determine whether all proteins

Molecular Pharmacology Fast Forward. Published on April 29, 2009 as DOI: 10.1124/mol.109.056085
This article has not been copyedited and formatted. The final version may differ from this version.

that enter the secretory pathway are downregulated, we also tested secreted protein osteonectin (SPARC) for changes by Western blot and did not detect any significant difference in protein levels (Figure 4D), indicating some degree of selectivity. We then compared these effects with responses induced by tunicamycin. For example, PDIs are known to be downregulated in response to tunicamycin, paralleling the effect of apratoxin A and in agreement with our previous data about the functional congruence between both compounds. The fingerprint (Table 1) suggested that apratoxin A affects the function of the ER, the site of glycoprotein synthesis. We then directly compared the regulation of selected validated proteins with the effect of tunicamycin on U2OS cells (Figure 4E). Like apratoxin A, tunicamycin induced the downregulation of RPN1. However, unlike the response to apratoxin A, CALR levels seemed slightly elevated after 24 h of tunicamycin treatment and BIP was strongly induced (Figure 4E), consistent with the induction of the unfolded protein response (Gülow et al., 2002). This response is opposite from the consequence of apratoxin A treatment (Figure 4D). This data indicated that the targets of both compounds are different while their mechanisms of action converge downstream.

Apratoxin A inhibits cotranslational processing *in vitro*. The downregulation of receptors and other proteins associated with the secretory pathway could be explained by inhibition of protein synthesis or by inhibition of processing including posttranslational modification. In the latter case, unprocessed or non-glycosylated proteins may quickly be degraded by the proteasome because of misfolding. The experiments in cell culture in which a proteasome inhibitor increased the intensity of nonglycosylated receptor suggested that this may be the case. To test this hypothesis and distinguish whether apratoxin A inhibits the synthesis of downregulated proteins or only downstream processing events, we turned to *in vitro* translation

Molecular Pharmacology Fast Forward. Published on April 29, 2009 as DOI: 10.1124/mol.109.056085
This article has not been copyedited and formatted. The final version may differ from this version.

with or without microsomal membrane and incorporating [^{35}S]methionine, followed by SDS-PAGE and autoradiography. Using α-factor mRNA as a standard substrate to assess effects of glycosylation, we determined that apratoxin A does not inhibit protein synthesis; however, glycosylation is inhibited even in the presence of microsomal membranes, as evidenced by the lack of the higher bands representing glycosylated forms (Figure 5A) (Hansen et al., 1986). The inhibition of α-factor glycosylation occurs in a dose-dependent manner, the IC_{50} being in 100-nM range (Figure 5B). To determine if apratoxin A also inhibits signal peptide cleavage, the event that precedes posttranslational modifications such as N-glycosylation, we used mRNA of β-lactamase as a substrate since the signal peptide-cleaved (processed) protein can be readily distinguished from the unprocessed form based on their migration by SDS-PAGE. As shown in Figure 5C, apratoxin A fully inhibits the cleavage of the signal peptide as no lower band for the processed form appears even in the presence of microsomal membranes. This inhibition also occurred in a dose-dependent fashion (Figure 5D). Subsequent treatment of the α-factor translation reactions with proteinase K (Hansen et al., 1986) revealed that the synthesized protein is unprotected from protease and thus synthesis is diverted to the cytoplasm (Figure 5E), in agreement with the proteasome inhibitor data presented above. In contrast (and as a control experiment), proteinase K had no effect on the glycosylated receptor since it was protected due to envelopment by the membrane. However, in the presence of detergent (1% Triton X-100) the membrane became permeable and proteinase K digested the fully processed receptor as well. We then showed by coupled *in vitro* transcription/translation using a more relevant mammalian cDNA template, that the glycosylation of a human receptor, PDGFR-β, is also inhibited *in vitro* in a similar fashion (Figure 5F).

Molecular Pharmacology Fast Forward. Published on April 29, 2009 as DOI: 10.1124/mol.109.056085
This article has not been copyedited and formatted. The final version may differ from this version.

Apratoxin A-induced loss of receptors and antiproliferative activity is reversible. To investigate the reversibility of apratoxin A-induced antiproliferative activity and ascertain when cells commit to apoptosis, we tested whether removal of medium several hours after apratoxin A treatment would affect its cell growth inhibitory activity and cytotoxicity (measured after 48 h). Clearly, the dose-response curve shifted towards higher GI_{50} and IC_{50} values when apratoxin A-treated U2OS cells are washed within 24 h (Figure 6A). Washout within the first 24 h could largely prevent cytotoxicity and only led to a transitory reduction in cell growth. Washout also prevented the induction of apoptosis as measured using Caspase-Glo 3/7 at concentrations of up to 100–300 nM, causing a shift in the dose-response curve by about 30-fold (Figure 6B). To determine if the recovery of the cells correlates with the potential re-appearance of receptors (or other secretory proteins), we carried out immunoblot analysis at various time points after washing (Figure 6C). For example, gp130 and PDGFR-β levels rapidly increased after medium exchange, strongly correlating with the cell viability and apoptosis results. With a certain lag period, Tyr705 phosphorylation of STAT3 was also restored over time (Figure 6C).

Discussion

The discovery of novel mechanisms of action is a vital task for pharmacotherapy. Natural products possess complex structures which presumably have evolved to exert effective interactions with their target biomolecules. While they are valid starting points for drug discovery, structurally unique natural products are likely to guide us towards discovering new modes of action as well. Based on published preliminary data that apratoxin A inhibits STAT3 phosphorylation and FGF signaling (Luesch et al., 2006), we have now further characterized the mode of action of this potent antiproliferative natural product and report here that apratoxin A

Molecular Pharmacology Fast Forward. Published on April 29, 2009 as DOI: 10.1124/mol.109.056085
This article has not been copyedited and formatted. The final version may differ from this version.

downregulates numerous cancer-associated receptors through inhibition of cotranslational translocation within the secretory pathway. Many of the identified membrane proteins are receptor tyrosine kinases (RTKs) that are validated targets for anticancer therapy associated with aberrant pro-growth signaling in cancer cells (Baselga, 2006). However, specific inhibitors of individual RTKs did not fulfill expectations with respect to therapeutic outcomes. Consequently, combination therapy using inhibitors for various RTKs may have cooperative beneficial effects (Kling, 2006). Rather than directly inhibiting the catalytic activity of these receptors, the mode of action of apratoxin A provides an alternative to achieve a potentially similar effect through simultaneous downregulation and consequent selective cellular depletion of these proteins.

These receptors, and also other membrane proteins and secreted proteins, originally contain N-terminal signal sequences that are required for targeting to the secretory pathway. After protein synthesis from such an mRNA template is initiated by free ribosomes, the signal recognition particle (SRP) binds to the signal sequence and exerts an elongation arrest which is released upon binding to the SRP receptor located in the ER (Walter et al., 1984). Continued protein synthesis is concomitant with translocation into the ER lumen in mammalian cells (cotranslational translocation), while protein translocation of membrane and other secretory proteins in yeast can occur through cotranslational or posttranslational translocation (Hansen et al., 1986). Signal peptides are then rapidly cleaved by cellular signal peptidases followed by additional processing by signal peptide peptidases (Lyko et al., 1995). Apratoxin A inhibits protein production at the stage of cotranslational translocation; synthesis of proteins that entered the secretory pathway occurs, yet is diverted to the cytoplasm where proteins are destined for rapid proteasomal degradation.

Molecular Pharmacology Fast Forward. Published on April 29, 2009 as DOI: 10.1124/mol.109.056085
This article has not been copyedited and formatted. The final version may differ from this version.

Apratoxin A is the first antitumor agent identified to act by this mechanism, consistent with the unique cytotoxicity profile in the NCI's 60 cell line screen. However, there is precedence for an anti-inflammatory fungal cyclodepsipeptide HUN-7293, minor variations of which known as cotransin and CAM741, act by a similar mechanism (Garrison et al, 2005; Besemer et al., 2005). Cotransin and CAM741 have a selectivity profile that is different from apratoxin A and mainly downregulate vascular cell adhesion molecule 1 (VCAM1) (Garrison et al, 2005; Besemer et al., 2005). Using photoaffinity labeling, cotransin's target was recently shown to be Sec61α (MacKinnon et al., 2007), an essential component of the translocon, which is sealed on the luminal end by BIP (downregulated by apratoxin A, Figure 4D) before and early in translocation (Hamman et al., 1998). The Sec61-containing translocon complex, particularly Sec61α, is one candidate target for apratoxins. Interfering with the SRP which could prevent SRP-induced elongation arrest could also explain the observations. However, the effect of apratoxin A on the function of the ER – even though much later than when translocation and processing are inhibited (Table 1 and Figure 4D) – may be suggestive of an ER component of the translocation machinery as the apratoxin A target. Upstream alternatives are the SRP complex, SRP receptor, or signal sequence since the cDNA sequences for at least several of the ER proteins (e.g., HYOU1, CANX, CALR) that are downregulated by apratoxin A predict an N-terminal signal sequence and rely on the signal recognition machinery. The protection assay (Figure 5E) suggests that signal peptidase is not the target of apratoxin A because otherwise membrane targeting and translocation would have been unaffected. The unambiguous target identification will likely require affinity-based methods which are currently being pursued in our laboratory.

In summary, we have shown that apratoxin A reversibly inhibits the secretory pathway for several cancer-associated receptors by interfering with their cotranslational translocation.

Molecular Pharmacology Fast Forward. Published on April 29, 2009 as DOI: 10.1124/mol.109.056085
This article has not been copyedited and formatted. The final version may differ from this version.

Apratoxin A shows nanomolar activity in cancer cells and in cell-free systems. Modulating the secretory pathway with apratoxin-based small molecules represents a new reversible method in live cells that may become a valuable new tool for investigating the secretory pathway. Apratoxin A selectivity needs to be further established and may be modulated through ongoing structure–activity relationship studies. This approach may have value for a variety of disease states where production of secretory or membrane proteins is involved and their downregulation would be beneficial.

Acknowledgments

We thank S. McClung and S. Chen for supporting the proteomics work, and T. Rowe, M. Law, N. Parker, P. Corsino and B. Davis for technical assistance.

Molecular Pharmacology Fast Forward. Published on April 29, 2009 as DOI: 10.1124/mol.109.056085
This article has not been copyedited and formatted. The final version may differ from this version.

References

Aggarwal K, Choe LH, and Lee KH (2006) Shotgun proteomics using the iTRAQ isobaric tags. *Brief Funct Genomic Proteomic* **5:**112–120.

Baselga J (2006) Targeting tyrosine kinases in cancer: the second wave. *Science* **312:**1175–1178.

Besemer J, Harant H, Wang S, Oberhauser B, Marquardt K, Foster CA, Schreiner EP, de Vries JE, Dascher-Nadel C, and Lindley IJD (2005) Selective inhibition of cotranslational translocation of vascular cell adhesion molecule 1. *Nature* **436:**290–293.

Blanchard F, Wang Y, Kinzie E, Duplomb L, Godard A, and Baumann H (2001) Oncostatin M regulates the synthesis and turnover of gp130, leukemia inhibitory factor receptor α, and oncostatin M receptor β by distinct mechanisms. *J Biol Chem* **276:**47038–47045.

Blunt JW, Copp BR, Hu WP, Munro MH, Northcote PT, and Prinsep MR (2008) Marine natural products. *Nat Prod Rep* **25:**35–94.

Bowman EJ and Bowman BJ (2005) V-ATPases as drug targets. *J Bioenerg Biomembr* **37:**431–435.

Chen J and Forsyth CJ (2004) Total synthesis of the marine cyanobacterial cyclodepsipeptide apratoxin A. *Proc Natl Acad Sci USA* **101:**12067–12072.

Chen SC, Chang YL, Wang DL, and Cheng JJ (2006) Herbal remedy magnolol suppresses IL-6-induced STAT3 activation and gene expression in endothelial cells. *Br J Pharmacol* **148:**226–232.

Doi T, Numarjiri Y, Munakata A, and Takahashi T (2006) Total synthesis of apratoxin A. *Org Lett* **8:**531–534.

Fenical W and Jensen PR (2006) Developing a new source for drug discovery: marine actinomycete bacteria. *Nat Chem Biol* **2:**666–673.

Garrison JL, Kunkel EJ, Hegde RS, and Taunton J (2005) A substrate-specific inhibitor of protein translocation into the endoplasmic reticulum. *Nature* **436:**285–289.

Garvin S, Nilsson UW, and Dabrosin C (2005) Effects of oestradiol and tamoxifen on VEGF, soluble VEGFR-1, and VEGFR-2 in breast cancer and endothelial cells. *Br J Cancer* **93:**1005–1010.

Gerwick WH, Tan LH, and Sitachitta N (2001) *Alkaloids Chem. Biol.* **57:**75–184.

Gutiérrez M, Suyama TL, Engene N, Wingerd JS, Matainaho T, and Gerwick WH (2008) Apratoxin D, a potent cytotoxic cyclodepsipeptide from Papua New Guinea collections of the marine cyanobacteria *Lyngbya majuscula* and *Lyngbya sordida*. *J Nat Prod* **71:**1099–1103.

Gülow K, Bienert D, and Haas IG (2002) Bip is feed-back regulated by control of protein translation efficiency. *J Cell Sci* **115:**2443–2452.

Hamman BD, Hendershot LM, and Johnson AE (1998) Bip maintains the permeability barrier of the ER membrane by sealing the luminal end of the translocon pore before and early in translocation. *Cell* **92:**747–758.

Hansen W, Garcia PD, and Walter P (1986) In vitro protein translocation across the yeast endoplasmic reticulum: ATP-dependent post-translational translocation of the prepro-α-factor. *Cell* **45:**397–406.

Heinrich PC, Behrmann I, Haan S, Hermanns HM, Müller-Newen G, and Schaper F (2003) Principles of interleukin (IL)-6-type cytokine signaling and its regulation. *Biochem J* **374:**1–20.

Johnson LS, Dunn KW, Pytowski B, and McGraw TE (1993) Endosome acidification and receptor trafficking: bafilomycin A_1 slows receptor externalization by a mechanism involving the receptor's internalization motif. *Mol Biol Cell* **4:**1251–1266.

Kawai A, Uchiyama H, Takano S, Nakamura N, and Ohkuma S (2007) Autophagosome-lysosome fusion depends on the pH in acidic compartments in CHO cells. *Autophagy* **3:**154–157.

Kling J (2006) Bundling next-generation cancer therapies for synergy. *Nat Biotechnol* **24:**871–872.

Liu L, McBride KM, and Reich NC (2005) STAT3 nuclear import is independent of tyrosine phosphorylation and mediated by importin-α3. *Proc Natl Acad Sci USA* **102:**8150–8155.

Luesch H, Yoshida WY, Moore RE, Paul VJ, and Corbett TH (2001) Total structure determination of apratoxin A, a potent novel cytotoxin from the marine cyanobacterium *Lyngbya majuscula*. *J Am Chem Soc* **123:**5418–5423.

Luesch H, Yoshida WY, Moore RE, and Paul VJ (2002) New apratoxins of marine cyanobacterial origin from Guam and Palau. *Bioorg Med Chem* **10:**1973–1978.

Luesch H, Chanda SK, Raya MR, DeJesus PD, Orth AP, Walker JR, Izpisúa Belmonte JC, and Schultz PG (2006) A functional genomics approach to the mode of action of apratoxin A. *Nat Chem Biol* **2:**158–167.

Lyko F, Martoglio B, Jungnickel B, Rapoport TA, and Dobberstein B (1995) Signal sequence processing in rough microsomes. *J Biol Chem* **270:**19873–19878.

Ma D, Zou B, Cai G, Hu X., and Liu JO (2006) Total synthesis of the cyclodepsipeptide apratoxin A and its analogues and assessment of their biological activities. *Chem Eur J* **12:**7615–7626.

MacKinnon AL, Garrison JL, Hegde RS, and Taunton J (2007) Photo-leucine incorporation reveals the target of a cyclodepsipeptide inhibitor of cotranslational translocation. *J Am Chem Soc* **129:**14560–14561.

Matthew S, Schupp PJ, and Luesch H (2008) Apratoxin E, a cytotoxic peptolide from a Guamanian collection of the marine cyanobacterium *Lyngbya bouillonii*. *J Nat Prod* **71:**1113–1116.

Nelson N, Cidon S, and Moriyama Y (1988) Chromaffin granule proton pump. *Methods Enzymol* **157:**619–633.

Newman DJ (2008) Natural products as leads to potential drugs: an old process or the new hope for drug discovery. *J Med Chem* **51:**2589–2599.

Nunomura K, Nagano K, Itagaki C, Taoka M, Okamura N, Yamauchi Y, Sugano S, Takahashi N, Izumi T, and Isobe T (2005) Cell surface labeling and mass spectrometry reveal diversity of cell surface markers and signaling molecules expressed in undifferentiated mouse embryonic stem cells. *Mol Cell Proteomics* **4:**1968–1976.

Shilov IV, Seymour SL, Patel AA, Loboda A, Tang WH, Keating SP, Hunter CL, Nuwaysir LM, and Schaeffer DA (2007) The Paragon algorithm, a next generation search engine that uses sequence temperature values and feature probabilities to identify peptides from tandem mass spectra. *Mol Cell Proteomics* **6:**1638–1655.

Taori K, Matthew S, Rocca JR, Paul VJ, and Luesch H (2007) Lyngbyastatins 5–7, potent elastase inhibitors from Floridian marine cyanobacteria, *Lyngbya* spp. *J Nat Prod* **70:**1593–1600.

Taori K, Paul VJ, and Luesch H (2008) Structure and activity of largazole, a potent antiproliferative agent from the Floridian marine cyanobacterium *Symploca* sp. *J Am Chem Soc* **130:**1806–1807.

Xiao G, Chung TF, Pyun HY, Fine RE, and Johnson RJ (1999) KDEL proteins are found on the surface of NG108-15 cells. *Brain Res Mol Brain Res* **72:**121–128.

Ying Y, Taori K, Kim H, Hong J, and Luesch H (2008) Total synthesis and molecular target of largazole, a histone deacetylase inhibitor. *J Am Chem Soc* **130:**8455–8459.

Walter P, Gilmore R, and Blobel G (1984) Protein translocation across the endoplasmic reticulum. *Cell* **38:**5–8.

Yuan ZL, GuanYJ., Chatterjee D, and Chin YE (2005) Stat3 dimerization regulated by reversible acetylation of a single lysine residue. *Science* **307:**269–273.

Zhong Z, Wen Z, and Darnell JE Jr (1994) Stat3: a STAT family member activated by tyrosine phosphorylation in response to epidermal growth factor and interleukin-6. *Science* **264:**95–98.

***** This work was financially supported by the James & Esther King Biomedical Research Program, Florida Department of Health, Grant No. 06-NIR07 (H.L.). Initial seed funding was provided through a Junior Investigator Award (pilot grant) from the University of Florida Shands Cancer Center, American Cancer Society, Institutional Research Grant, ACS-IRG-01-188-01 (H.L.).

Molecular Pharmacology Fast Forward. Published on April 29, 2009 as DOI: 10.1124/mol.109.056085
This article has not been copyedited and formatted. The final version may differ from this version.

Figure legends

Fig. 1. Effects of apratoxin A on STAT3 signaling in U2OS cells. A, Structure of apratoxin A. B, Apratoxin A promotes STAT3 nuclear translocation as determined by immunoblot analysis using U2OS nuclear extracts. Levels of the nuclear protein OCT1 did not change and cytoplasmic contamination was minimal based on probing with β-tubulin (TUBB) antibody. C, Apratoxin A inhibits JAK1/JAK2 phosphorylation at the catalytic tyrosine residues as determined by immunoblot analysis using whole cell protein extracts. Total JAK1 and JAK2 protein levels were largely unaffected. D, STAT3 (Tyr705) phosphorylation is strongly induced by IL-6 in U2OS cells. U2OS cells were first serum-starved for 48 h to reduce the level of (FBS-mediated) constitutive STAT3 (Tyr705) phosphorylation and then stimulated with IL-6 for 20 or 60 min at various cytokine concentrations. Total proteins were isolated with PhosphoSafe lysis buffer, subjected to SDS-PAGE and Western blot analysis. Optimal conditions from this experiment leading to strongly increased STAT3 (Tyr705) phosphorylation (20 min, 10 ng/mL IL-6) were used in subsequent experiments. E, Apratoxin A inhibits IL-6 induced STAT3 (Tyr705) phosphorylation in pretreated U2OS cells. Conditions from panel D were adopted. Serum-starved U2OS cells were pretreated with 5 or 50 nM of apratoxin A for the indicated times before stimulation with IL-6, isolation of total proteins, and Western blot analysis as above. Apratoxin A prevented IL-6 mediated STAT3 (Tyr705) phosphorylation but only when cells were pretreated for 4 h or longer. Pretreatment for 1 h was not sufficient. F, Apratoxin A depletes gp130 from U2OS cells concomitant with the reduction of STAT3 (Tyr705) phosphorylation as determined by immunoblot analysis. G, RNAi-mediated depletion of gp130 in U2OS cells is associated with the inhibition of STAT3 (Tyr705) phosphorylation. U2OS cells

Molecular Pharmacology Fast Forward. Published on April 29, 2009 as DOI: 10.1124/mol.109.056085
This article has not been copyedited and formatted. The final version may differ from this version.

were transfected with two individual *gp130*-specific siRNA (or one control siRNA) mediated by siLentFect (Bio-Rad), 48 h later total proteins were extracted and SDS-PAGE resolved proteins analyzed by Western blotting for siRNA efficacy and effects on STAT3 phosphorylation status using anti-gp130 and anti-STAT3 (Tyr705) antibodies, respectively. STAT3 levels were unchanged. Blots in panels B–G are representative of at least three experiments with similar results.

Fig. 2. Effect of apratoxin A on *gp130* mRNA levels and gp130 protein degradation. A, Apratoxin A has no considerable effect on *gp130* transcript levels. U2OS cells were treated with apratoxin A (50 nM), total RNA was isolated after various exposure times, reverse-transcribed to cDNA, and subjected to TaqMan analysis (n = 3). *GAPDH* was used as internal control for normalization. B, Effect of proteasome inhibition on apratoxin A-mediated gp130 depletion. U2OS cells were pretreated with the proteasome inhibitor MG132 (1 μM) or vehicle control for 30 min before exposure to apratoxin A (50 nM) for 2, 4 or 8 h. Total proteins were isolated, resolved by SDS-PAGE and subjected to immunoblot analysis. An immunoreactive gp130 band was increased in intensity when pretreated with MG132. The phosphorylation of STAT3 was not affected. A representative blot from three experiments with similar results is shown. C,D, Effect of lysosome inhibition on apratoxin A-mediated gp130 depletion. U2OS cells were either pretreated with (C) NH_4Cl (20 mM) for 2 h or (D) chloroquine (100 μM) for 30 min, followed by treatment with apratoxin A (50 nM) for the indicated times. Total proteins were isolated, resolved by SDS-PAGE and subjected to immunoblot analysis. Lysosome inhibition slightly attenuated the effects of apratoxin A on gp130 levels, while the lower immunoreactive band was not stabilized. Rescue effects with respect to STAT3 phosphorylation were marginal. Results are

Molecular Pharmacology Fast Forward. Published on April 29, 2009 as DOI: 10.1124/mol.109.056085
This article has not been copyedited and formatted. The final version may differ from this version.

representative of three experiments with similar results. E, Effects of apratoxin A and bafilomycin A_1 on the pH of acidic compartments (lysosome). U2OS cells were seeded in 96-well plates. The next day, cells were incubated with LysoTracker Red (Invitrogen) at 37 °C (final concentration 500 nM) to mark the acidic lysosome, 30 min later the medium was removed and the cells were washed twice with PBS and wells refilled with culture medium. The cells were treated with apratoxin A (10 nM, 100 nM and 1 μM) or bafilomycin A_1 (5 nM, 50 nM and 500 nM) or solvent controls (EtOH or DMSO, respectively) for 3 h. The medium was washed out and wells refilled with PBS, images were captured under a fluorescence microscope (Eclipse Ti, Nikon, Japan). While the red fluorescence disappears with increasing concentration of bafilomycin A_1 due to alkalinization, apratoxin A did not affect the lysosomal pH (scale bar: 30 μm). Results are representative of three experiments with similar results.

Fig. 3. Effect of apratoxin A on receptor levels and N-linked glycosylation. A, Apratoxin A downregulates several cancer-associated receptors as determined by immunoblot analysis. U2OS cells were treated with apratoxin A for the indicated times, whole-cell lysates prepared and proteins resolved by SDS-PAGE, transferred to PVDF membranes which were then blotted with various receptor antibodies. Consistently, for all receptors a new faster migrating immunoreactive band of varying intensity appeared in apratoxin A treated samples. B, Effect of the N-glycosylation inhibitor tunicamycin on various receptors and STAT3 phosphorylation in comparison with apratoxin A. U2OS cells were treated with tunicamycin (500 ng/mL) and subjected to immunoblot analysis as described for panel A. The effects of tunicamycin and apratoxin A are identical in this analysis. C, Effect of the protein synthesis inhibitor

Molecular Pharmacology Fast Forward. Published on April 29, 2009 as DOI: 10.1124/mol.109.056085
This article has not been copyedited and formatted. The final version may differ from this version.

cycloheximide on various receptors and STAT3 phosphorylation in comparison with apratoxin A. The same analysis as described for panel B was carried out for cells treated with cycloheximide (1 μg/mL). While receptors also rapidly disappeared, cycloheximide treatment did not cause the faster migrating band to appear as tunicamycin or apratoxin A. D, Direct comparison of apratoxin A treatment and apratoxin A cotreatment with tunicamycin or cycloheximide. U2OS cells were treated with apratoxin A (50 nM) or additionally supplemented with either tunicamycin (500 ng/mL) or cycloheximide (1 μg/mL). Protein lysates from various time points were analyzed for gp130 by immunoblot analysis as described above. E, Effect of apratoxin A on the degradation rate of pre-existing gp130. U2OS cells were biotinylated with with Sulfo-NHS-SS-Biotin (4 ^{o}C for 30 min) and then (t_0) incubated with apratoxin A (50 nM) or vehicle (0.25% ethanol) for the indicated times. Protein lysates were prepared and an aliquot analyzed for total gp130 and STAT3 by immunoblot analysis. Biotinylated proteins from the remaining lysates were isolated using Neutravidin Gel followed by cleavage of the tag and elution with DTT. The enriched cell surface proteins were separated by SDS-PAGE (4–12%) and analyzed for gp130 by immunoblot analysis. No differences were apparent between control and apratoxin A treated cells with respect to the degradation of pre-existing cell surface gp130. F, Effect of apratoxin A on growth factor receptors in MCF7 cells as determined by immunoblot analysis. VEGFR2 and FGFR2 levels were strongly reduced upon 12 h of apratoxin A treatment. G, Apratoxin A downregulates several plasma membrane proteins within 12 h. U2OS cells treated with apratoxin A or control for 12 h were lysed by hypotonic treatment and cell rupture, plasma membrane proteins were isolated by sucrose density gradient ultracentrifugation as described in Materials and Methods, resolved by SDS-PAGE (4–12%) followed by immunoblot analysis (anti-PDFGR-β) to verify receptor enrichment or silver staining for total protein (lanes 3

Molecular Pharmacology Fast Forward. Published on April 29, 2009 as DOI: 10.1124/mol.109.056085
This article has not been copyedited and formatted. The final version may differ from this version.

and 4). For comparison, lanes 1 and 2 contain total cellular proteins derived from apratoxin A-treated or control cells. Effects of apratoxin A can be discerned in the plasma membrane fraction (indicated by *) but not in whole-cell lysates. H, Apratoxin A reduces levels of several N-glycosylated proteins. U2OS cells were treated with apratoxin A for 12 or 24 h, membrane proteins were isolated and enriched in N-glycoproteins by affinity capture with Concanavalin A-agarose and recovered by subsequent selective elution with 0.5 M methyl-α-D-mannopyranoside. Samples were resolved by SDS-PAGE (4–12%) and subjected to immunoblot analysis (anti-gp130) to verify glycoprotein enrichment compared with whole-cell lysates (lanes 1 and 2). Another sample set was used for silver staining, revealing marked reductions in a subset of N-glycoproteins (indicated by *). Results are representative of at least three experiments with similar results.

Fig. 4. Proteomics reveals additional effects of apratoxin A on receptors and the ER. A, Method for iTRAQ-based quantification of whole-cell proteome or cell surface protein enriched proteomics. U2OS cells were treated with apratoxin A or vehicle control for 1, 4, 12 or 24 h. Either total proteins were extracted (middle) or cells were biotinylated with Sulfo-NHS-SS-Biotin (**2**) at 4 ^{o}C for 30 min, lysed, and biotinylated proteins enriched by NeutrAvidin-agarose binding and subsequent DTT-mediated disulfide cleavage (right). In both scenarios proteins are precipitated, digested and labeled with 8-plex isobaric iTRAQ reagents according to the manufacturer's protocol (Applied Biosystems). The eight labeled digests from each approach were combined, fractionated by cation exchange and analyzed by reversed-phase (C18) HPLC-MS/MS. Peptides and parent proteins were identified and quantified based on iTRAQ labels by ProteinPilot analysis. Subsequent validation is described in panel D. Each proteomic analysis

Molecular Pharmacology Fast Forward. Published on April 29, 2009 as DOI: 10.1124/mol.109.056085
This article has not been copyedited and formatted. The final version may differ from this version.

was carried out one time. B,C Validation of biotinylation. Lysates from biotinylated cells were separated by SDS-PAGE (4–12%) and subjected to Western blot analysis (B) before NeutrAvidin-agarose incubation, probing for biotin with streptavidin-HRP which indicated high level of biotinylation in the mid to high molecular weight range, and (C) after DTT-mediated elution from NeutrAvidin, probing for gp130 levels which indicated a strong enrichment. Panel C also shows a silver stained SDS-PAGE gel revealing some minor differences between apratoxin A and control samples (indicated by *). For comparison, whole-cell lysate analysis is included in the left lanes (lanes 1 and 2). Immunoblot (B) and silver staining (C) analyses are representative of two and three experiments, respectively. D, Validation of proteomics results: apratoxin A reduces levels of several ER proteins. U2OS cells were treated with apratoxin A or control for 1, 4, 12 or 24 h, whole-cell lysates collected, and total cellular proteins resolved by SDS-PAGE and subjected to immunoblot analysis for various ER proteins from Table 1. As a control, apratoxin A did not change SPARC levels. E, Tunicamycin's effects on components of the ER are different from the effect of apratoxin A. A similar analysis as in panel D, using U2OS cells treated with tunicamycin (500 ng/mL) and probing for ER proteins that are reduced upon apratoxin A treatment (CALR, BIP, RPN1), indicated that CALR levels are unaffected by tunicamycin and BIP levels strongly increased, while RPN1 levels are decreased as for apratoxin A. Blots in panels D and E are representative of three experiments with similar results.

Fig. 5. Apratoxin A inhibits cotranslational translocation *in vitro*. For *in vitro* translation reactions (A–E), rabbit reticulocyte lysate, amino acid mix (minus methionine), [^{35}S]methionine, and mRNA substrate were incubated in the presence or absence of canine pancreatic microsomal membranes with apratoxin A or solvent control. Samples were resolved by SDS-PAGE (20% for

Molecular Pharmacology Fast Forward. Published on April 29, 2009 as DOI: 10.1124/mol.109.056085
This article has not been copyedited and formatted. The final version may differ from this version.

panels A–E and 7.5% for panel F), proteins transferred to nitrocellulose membranes and detected by autoradiography. A,B, Effect of apratoxin A on *in vitro* translation and glycosylation of α-factor mRNA. In the absence of microsomal membranes (A, left lanes: 1 and 2), α-factor is synthesized regardless of the presence of apratoxin A (10 μM). In the presence of microsomal membranes (A, right lanes: 3 and 4) apratoxin A (10 μM) inhibits the glycosylation of α-factor. This inhibition occurs in a dose-dependent fashion (B) with an approximate IC_{50} of 100 nM. C,D, Effect of apratoxin A on *in vitro* translation of β-lactamase mRNA and subsequent signal peptide cleavage (processing). While apratoxin A does not interfere with the synthesis of β-lactamase (C, no membrane, left lanes: 1 and 2), it inhibits the cleavage of the signal peptide (C, lane 4) which is usually observed after incubation with microsomal membranes (C, lane 3). (D) This inhibition is dose-dependent (IC_{50} between 100 nM to 1 μM). E, Protease protection: apratoxin A diverts protein synthesis to the cytoplasm. Proteinase K readily digests non-glycosylated (precursor) α-factor (lane 2) but glycosylated proteins only in the presence of detergent (Triton X-100, lane 3). In the presence of apratoxin A, α-factor is degraded and thus not effectively inserted into the membrane. F, Apratoxin A inhibits glycosylation of a mammalian receptor *in vitro*. *In vitro* transcription/translation was carried out using the T7 TNT Quick Master Mix, PDGFR-β plasmid cDNA, canine microsomal membranes, [^{35}S]methionine and apratoxin A or solvent control. Subsequently, samples were resolved by SDS-PAGE, proteins transferred to nitrocellulose membranes and detected by autoradiography. Apratoxin A does not affect the synthesis of PDGFR-β, but it prevents its glycosylation in a dose-response manner (IC_{50} ~ 100 nM). Results are representative of at least two experiments with similar results.

Molecular Pharmacology Fast Forward. Published on April 29, 2009 as DOI: 10.1124/mol.109.056085
This article has not been copyedited and formatted. The final version may differ from this version.

Fig. 6. The effects of apratoxin A are reversible. U2OS cells were treated with various concentrations of apratoxin A for 1, 4, 12 and 24 h, the medium was removed, cells washed once and replenished with fresh medium. A, Removal of apratoxin A within several hours of treatment attenuates its effect on cell viability. Cell viability was measured using the MTT assay 48 h after the beginning of apratoxin A treatment. For comparison, a dose-response for continuous 48 h-exposure was included in parallel. IC_{50} and GI_{50} values are 10- to 33-fold higher if medium containing apratoxin A is replaced with fresh medium within 1 to 24 h (IC_{50}: concentration at which the cell viability is 50%; GI_{50}: concentration at which the cell growth is inhibited by 50%). When cells were washed at any of the time points, there was only marginal cytotoxicity observed at higher concentrations. Experiments were carried out in triplicate. Values are presented as mean ± standard deviation. B, Removal of apratoxin A within several hours of treatment prevents apoptosis. Caspase 3/7 activity was measured using the Caspase-Glo 3/7 kit (Promega) 48 h after initial exposure to apratoxin A. For comparison, a dose-response analysis was included where cells have been continuously exposed to apratoxin A for 48 h. Dose-response curves are shifted by ~30-fold and residual caspase 3/7 activity may be attributed to incomplete removal of apratoxin A-containing medium. Error bars indicate standard deviations from mean of three independent experiments. C, The effects of apratoxin A on receptor levels are reversible. After apratoxin A washout, cells were further incubated with fresh medium and total proteins collected using PhosphoSafe lysis buffer 1, 4, 12, 24, 48, 72 or 96 h after the beginning of apratoxin A treatment. Proteins were resolved by SDS-PAGE and subjected to Western blot analysis. Receptor levels (gp130, PDGFR-β) recovered and at later time points the phosphorylation of STAT3 was partially or completely restored. Blots are representative of at least two experiments with similar results.

Molecular Pharmacology Fast Forward. Published on April 29, 2009 as DOI: 10.1124/mol.109.056085
This article has not been copyedited and formatted. The final version may differ from this version.

TABLE 1. Selected apratoxin A (50 nM) induced fold changes in levels of proteins enriched after cell surface biotinylation of U2OS cells (quantified by iTRAQ labeling)[a]

Gene Symbol	Annotation	Peptides[b]	1 h	4 h	12 h	24 h
Receptors/cell surface proteins						
LRPAP1	low density lipoprotein receptor-related protein associated protein 1	8	–1.13	**–1.61**	**–4.06**	**–3.79**
M6PR	mannose-6-phosphate receptor (cation dependent)	4	+1.02	–1.07	**–2.70**	**–1.54**
CD151	CD151 molecule (Raph blood group)	1	–1.01	+1.02	**–2.63**	**–1.37**
GPC1	glypican 1	7	+1.36	+1.02	**–2.21**	**–1.65**
ITGAV	integrin, alpha V (vitronectin receptor, alpha polypeptide)	21	+1.15	–1.03	**–2.04**	**–1.76**
TFRC	transferrin receptor (p90, CD71)	28	+1.01	–1.25	**–1.83**	**–2.79**
DAG1	dystroglycan 1 (dystrophin-associated glycoprotein 1)	13	–1.09	–1.25	**–1.71**	**–2.26**
ITGB1	integrin, beta 1 (fibronectin receptor, beta polypeptide)	20	–1.06	–1.06	**–1.56**	**–1.98**
CCDC47	coiled-coil domain containing 47	4	+1.07	+1.38	–1.35	**–13.87**
ANXA1	annexin A1	5	+1.61	–1.12	**+2.01**	**+1.81**
Protein disulfide isomerases						
PDIA3	protein disulfide isomerase family A, member 3	23	+1.10	+1.15	**–1.65**	**–3.02**
PDIA4	protein disulfide isomerase family A, member 4	17	–1.04	+1.17	**–1.93**	**–4.15**
PDIA6	protein disulfide isomerase family A, member 6	12	–1.15	–1.04	**–1.71**	**–2.86**
TXNDC4	thioredoxin domain containing 4 (endoplasmic reticulum)	7	+1.10	–1.13	**–1.78**	**–2.14**
TXNDC5	thioredoxin domain containing 5	8	+1.13	+1.31	**–1.88**	**–3.20**
Other ER proteins						
CALU	calumenin	8	–1.19	+1.11	**–2.52**	**–5.08**
RCN1	reticulocalbin 1, EF-hand calcium binding domain	8	–1.08	+1.04	**–2.39**	**–5.87**

Molecular Pharmacology Fast Forward. Published on April 29, 2009 as DOI: 10.1124/mol.109.056085
This article has not been copyedited and formatted. The final version may differ from this version.

RCN2	reticulocalbin 2, EF-hand calcium binding domain	5	–1.14	–1.15	**–2.13**	**–2.14**
HSPA5 (BIP)	heat shock 70kDa protein 5 (glucose-regulated protein, 78kDa)	28	–1.02	+1.08	**–2.08**	**–3.70**
LMAN1	lectin, mannose-binding, 1	11	–1.09	–1.13	**–2.03**	**–2.67**
HYOU1	hypoxia up-regulated 1	27	–1.14	+1.24	**–2.02**	**–3.02**
CANX	calnexin	14	–1.08	–1.12	**–2.02**	**–3.21**
HSP90B1	heat shock protein 90kDa beta (Grp94), member 1	38	±1.00	+1.15	**–1.95**	**–3.11**
STT3A	STT3, subunit of the oligosaccharyltransferase complex, homolog A (S. cerevisiae)	8	+1.31	–1.11	**–1.90**	**–1.99**
RPN1	ribophorin I	13	–1.06	–1.13	**–1.77**	**–2.23**
PPIB	peptidylprolyl isomerase B (cyclophilin B)	14	–1.05	+1.36	**–1.75**	**–3.32**
CALR	calreticulin	12	–1.15	+0.82	**–1.69**	**–3.46**
GANAB	glucosidase, alpha; neutral AB	27	–1.06	+1.24	**–1.64**	**–3.12**
UGCGL1	UDP-glucose ceramide glucosyltransferase-like 1	17	–1.28	–1.08	–1.06	**–2.77**
tRNA synthetases & protein biosynthesis						
RARS	arginyl-tRNA synthetase	13	+1.04	–1.02	**+1.43**	**+2.21**
QARS	glutaminyl-tRNA synthetase	15	–1.20	–1.15	**+1.44**	**+1.47**
DARS	aspartyl-tRNA synthetase	9	–1.06	–1.15	**+1.56**	**+1.85**
KARS	lysyl-tRNA synthetase	15	+1.06	+1.07	**+1.59**	**+1.41**
TARS	threonyl-tRNA synthetase	11	–1.35	+1.13	**+1.86**	**+1.29**
IARS	isoleucyl-tRNA synthetase	21	+1.63	–1.04	**+2.02**	**+1.69**
RPL12	ribosomal protein L12	3	+1.27	+1.66	**+2.32**	**+2.15**
EIF3D	eukaryotic translation initiation factor 3, subunit D	3	–1.61	–1.43	**+2.39**	+1.11
SRP72	signal recognition particle 72kDa	12	+1.32	–1.08	**+2.55**	**+1.50**

[a] 95% confidence level. [b] Used for protein identification.

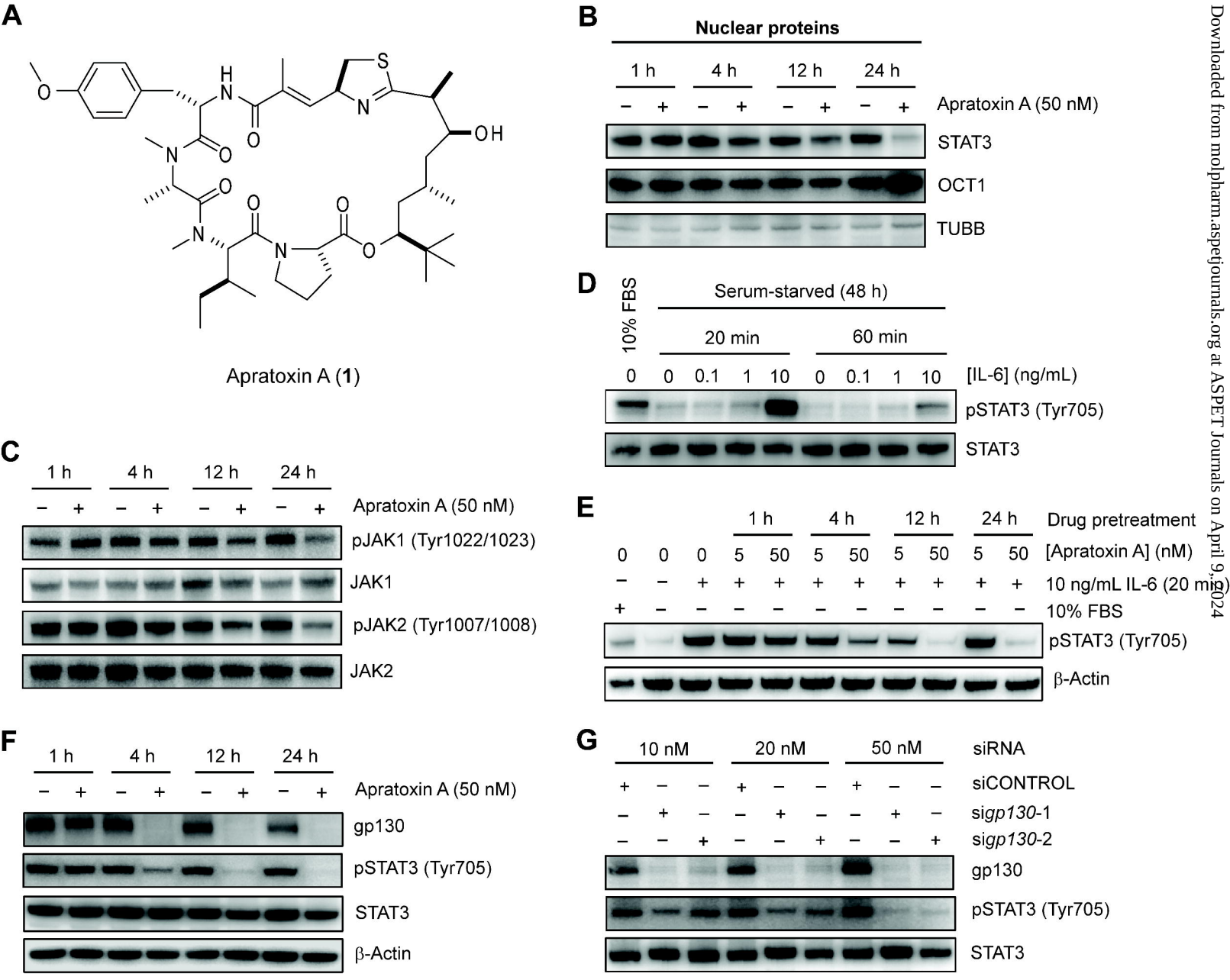

Figure 1

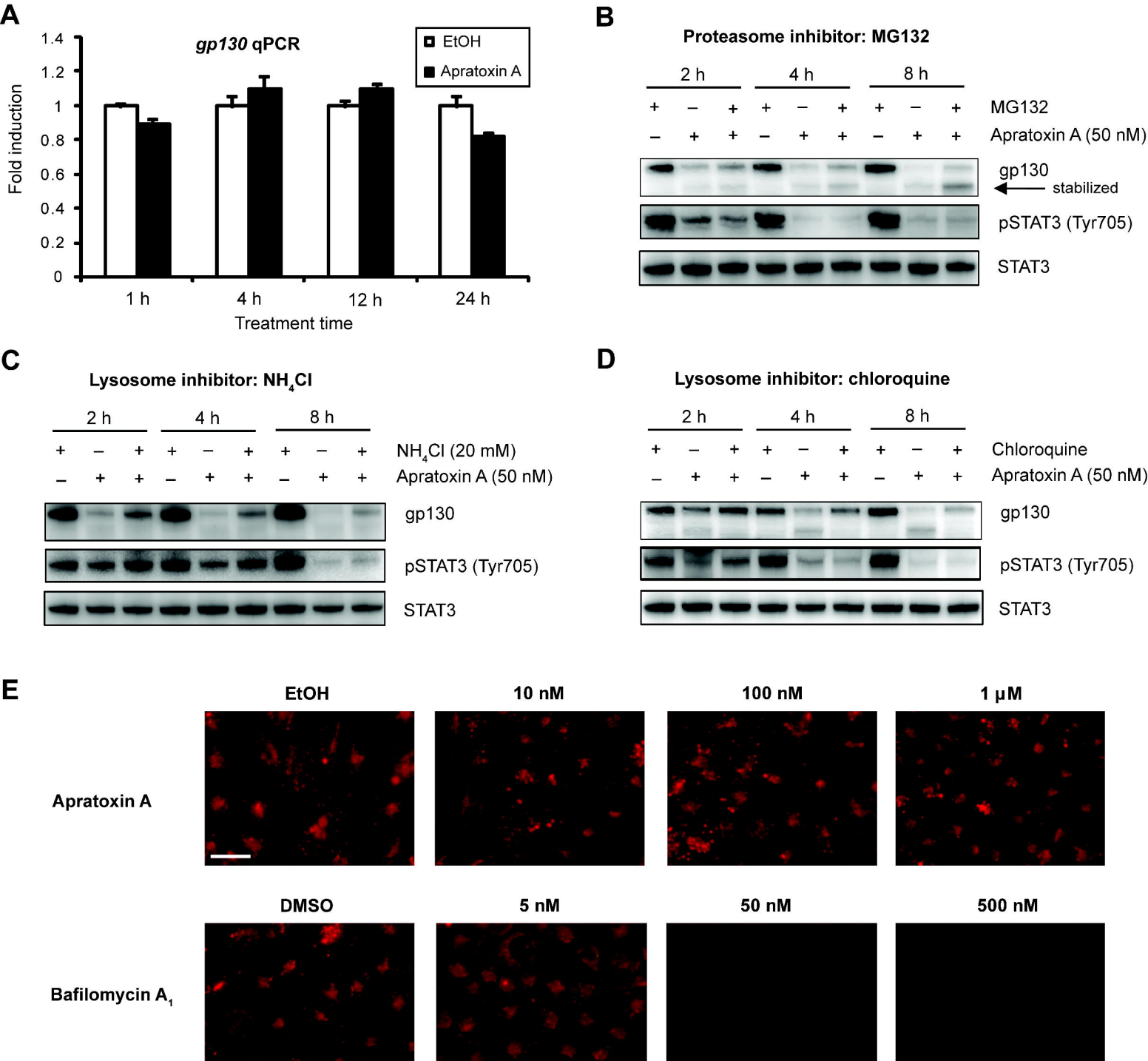
A
gp130 qPCR
EtOH
Apratoxin A
Fold induction
1.4
1.2
1
0.8
0.6
0.4
0.2
0
1 h
4 h
12 h
24 h
Treatment time
B
Proteasome inhibitor: MG132
2 h
4 h
8 h
MG132
Apratoxin A (50 nM)
gp130
stabilized
pSTAT3 (Tyr705)
STAT3
C
Lysosome inhibitor: NH4Cl
NH4Cl (20 mM)
Apratoxin A (50 nM)
gp130
pSTAT3 (Tyr705)
STAT3
D
Lysosome inhibitor: chloroquine
Chloroquine
Apratoxin A (50 nM)
gp130
pSTAT3 (Tyr705)
STAT3
E
EtOH
10 nM
100 nM
1 µM
Apratoxin A
DMSO
5 nM
50 nM
500 nM
Bafilomycin A1

Figure 2

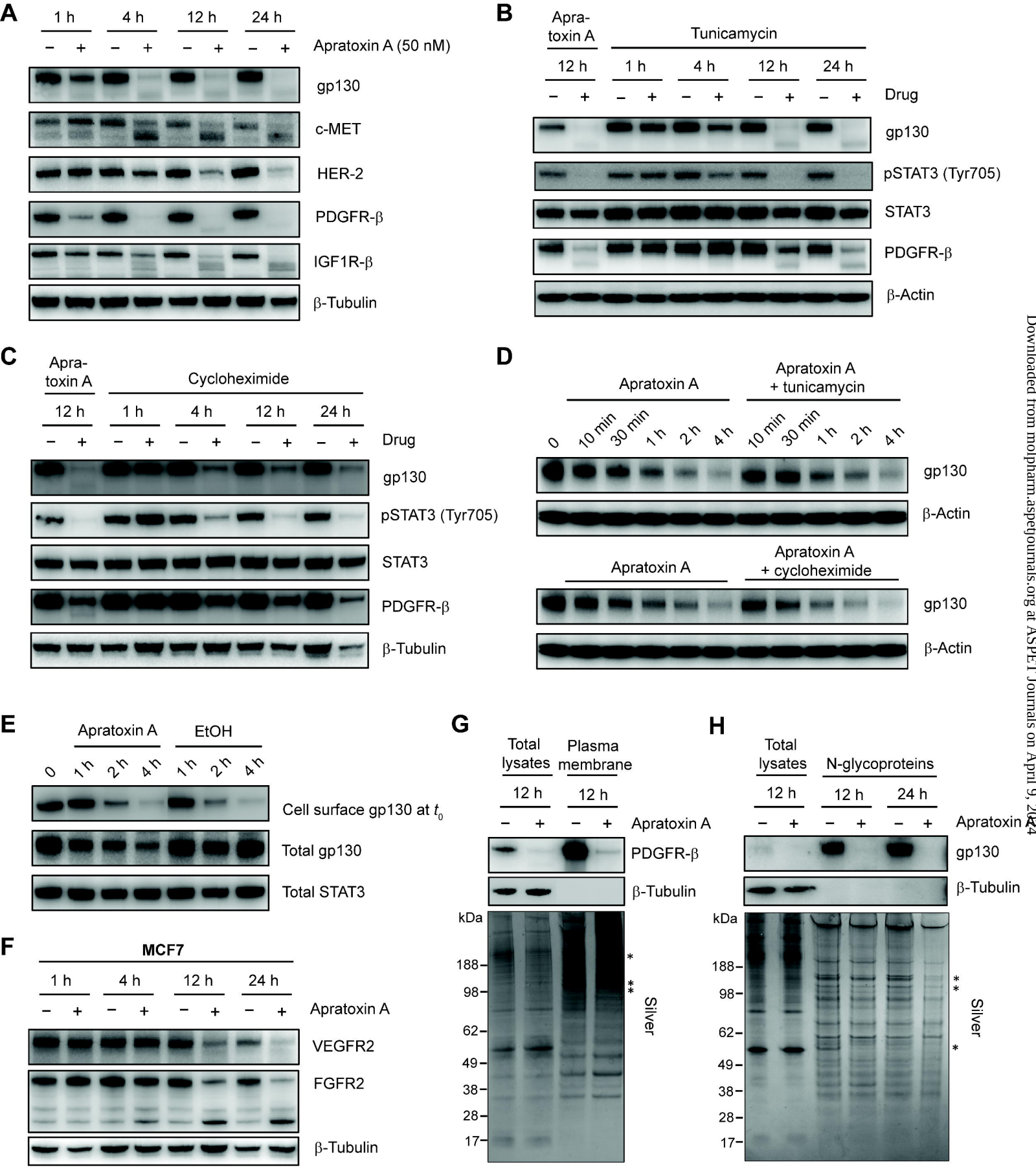

Figure 3

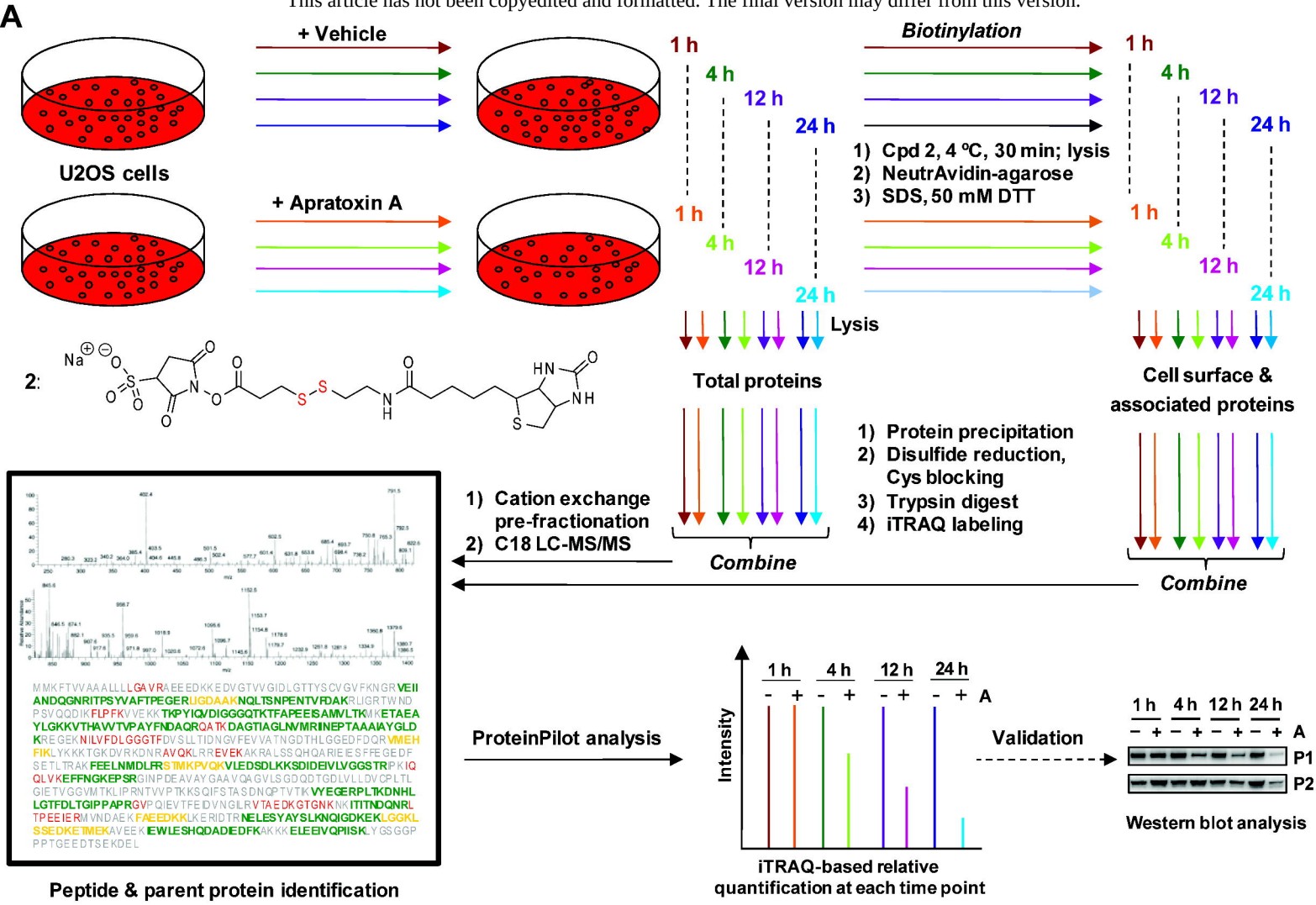

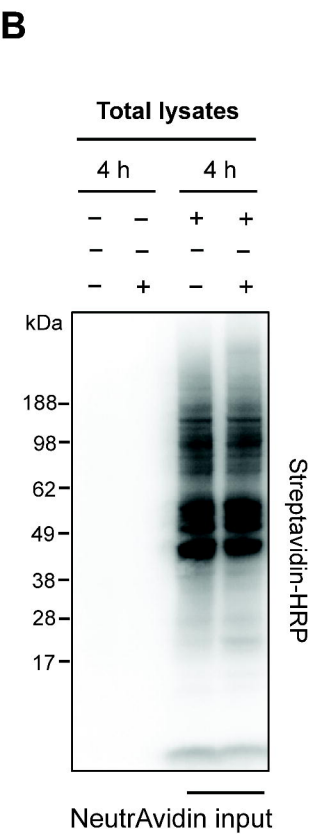

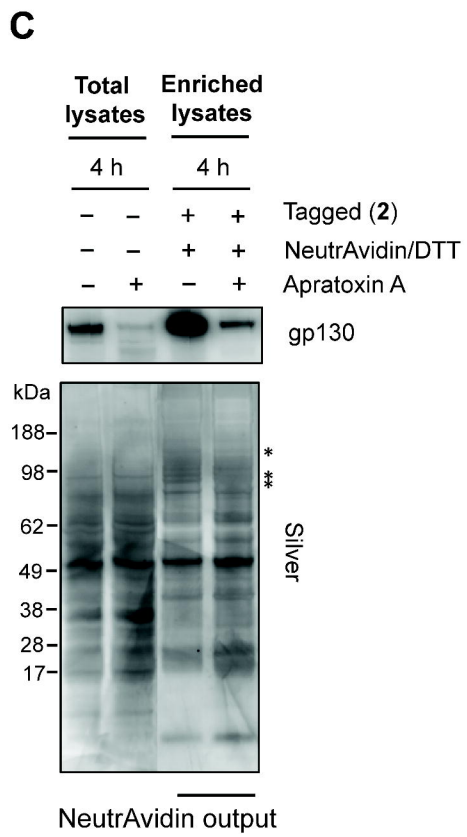

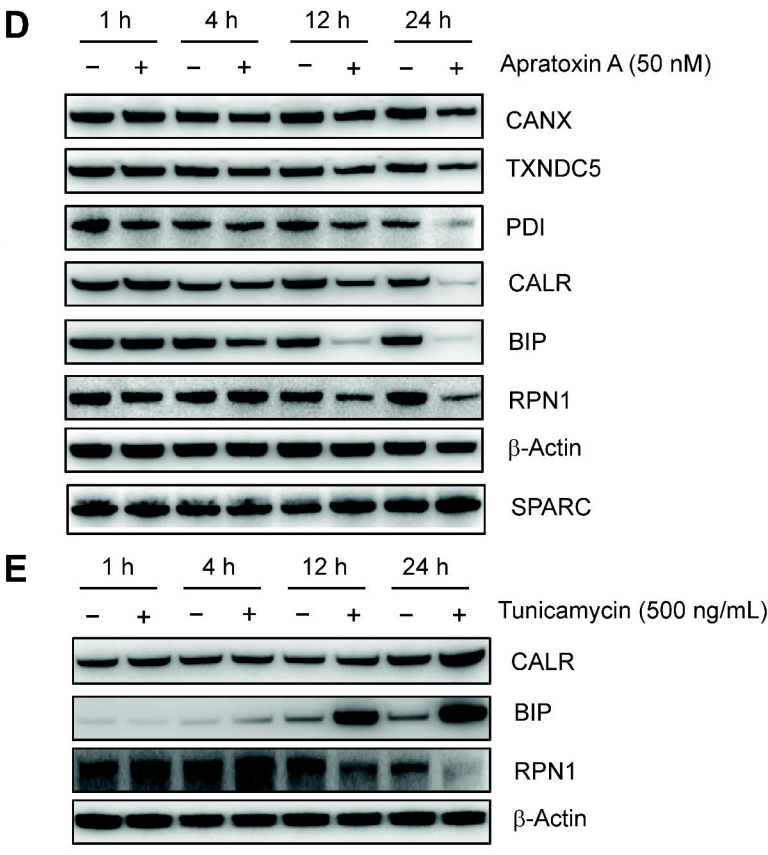

Figure 4

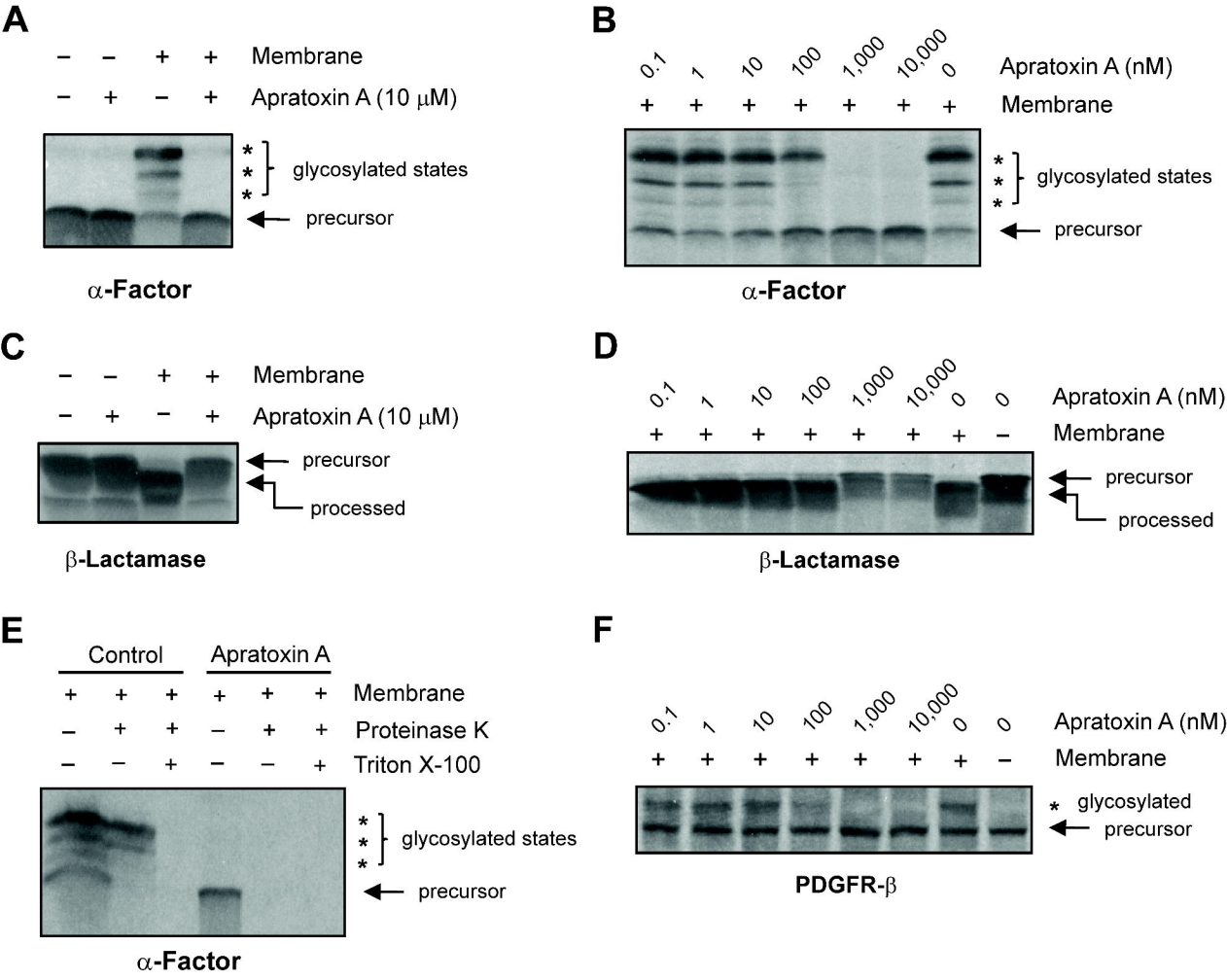
A
– – + + Membrane
– + – + Apratoxin A (10 μM)
glycosylated states
precursor
α-Factor
B
0.1 1 10 100 1,000 10,000 0
Apratoxin A (nM)
+ + + + + + + Membrane
glycosylated states
precursor
α-Factor
C
– – + + Membrane
– + – + Apratoxin A (10 μM)
precursor
processed
β-Lactamase
D
0.1 1 10 100 1,000 10,000 0 0
Apratoxin A (nM)
+ + + + + + + – Membrane
precursor
processed
β-Lactamase
E
Control
Apratoxin A
+ + + + + + Membrane
– + + – + + Proteinase K
– – + – – + Triton X-100
glycosylated states
precursor
α-Factor
F
0.1 1 10 100 1,000 10,000 0 0
Apratoxin A (nM)
+ + + + + + + – Membrane
glycosylated
precursor
PDGFR-β

Figure 5

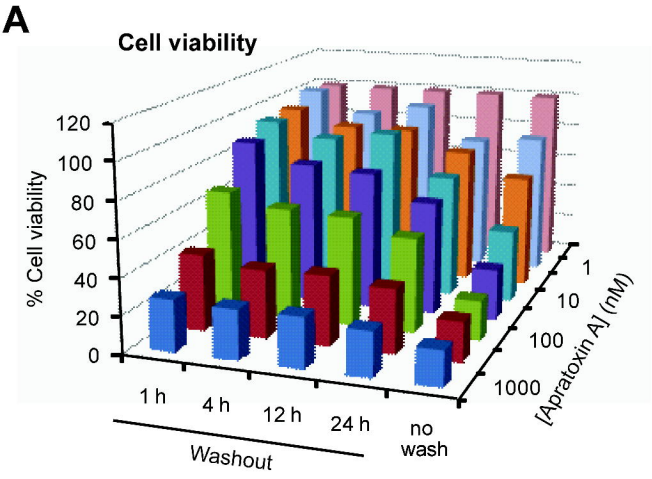

Wash	IC_{50} (nM)	GI_{50} (nM)
1 h	205 ± 7	116 ± 20
4 h	157 ± 5	89 ± 9
12 h	147 ± 25	76 ± 23
24 h	85 ± 1	29 ± 1
no wash	6.7 ± 0.7	3.5 ± 0.7

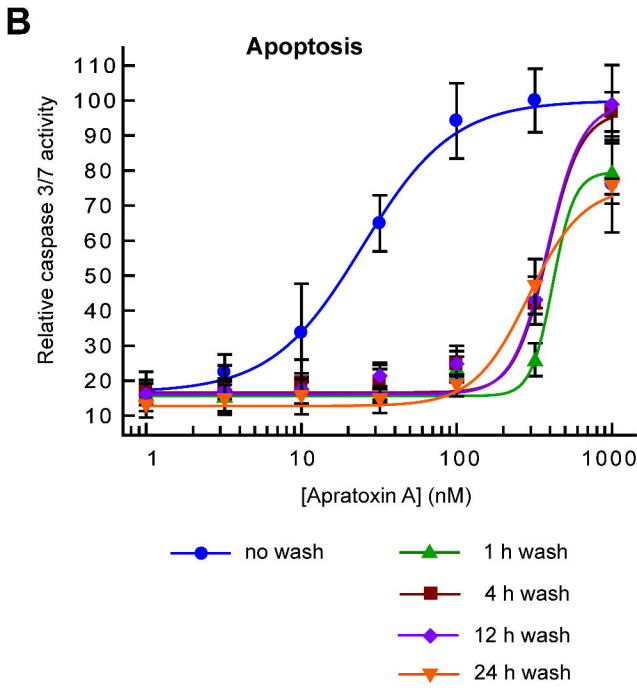

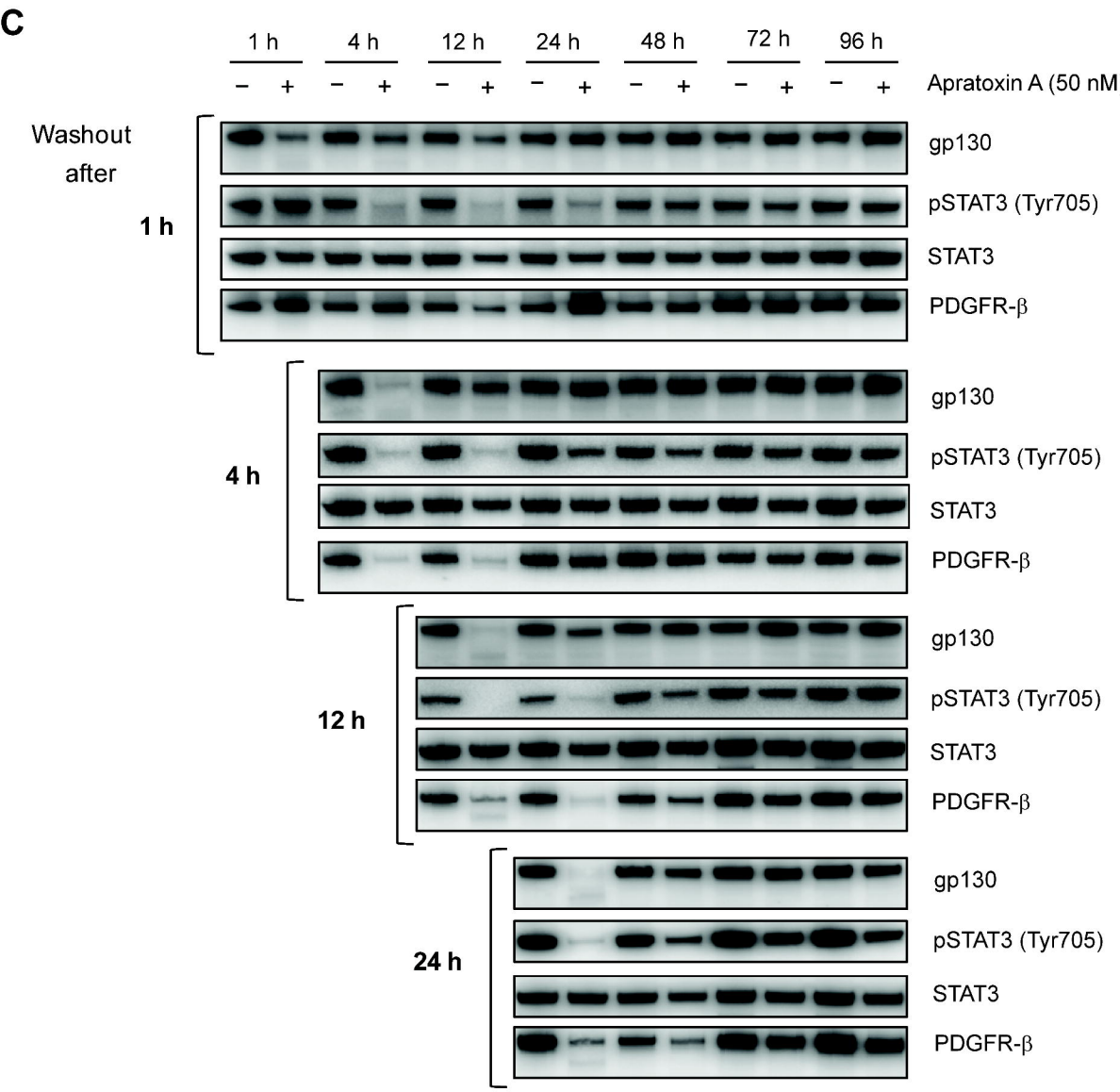

Figure 6